Sup-norm stability radii for a nodal face of the B_3 spherical discriminant

Oleksiy Babanskyy

Abstract

How large can a real perturbation be before a nodal line ceases to be a single graph in a fixed spherical sector? We study a truncated face of the degree-nine B_3 discriminant, allowing all 100 real spherical polynomial modes of degree at most nine and measuring the supremum norm on the entire closed tube. The failure radius equals the minimum cost of cancelling the field and its normal derivative. We bound it on the full parameter domain and determine it exactly in two sufficient regimes, using an explicit atomic mixed-jet certificate on the sphere. In these exact regimes the unique critical field is a scaled Chebyshev polynomial, and the whole closed radius ball still preserves the graph, although the critical zero level is singular; every larger amplification of that field fails. Two continuous examples separate the limits of a support criterion from those of the radius formula. Below the radius we obtain quantitative graph bounds. In the exact regimes a smooth family approaching the critical field from inside the ball has uniformly convergent graphs and terminal slopes diverging as $\varepsilon^{-1/3}$ at the minimizing terminals. Persistence and C^1 conditioning therefore separate.

1 Introduction

The zero set of a signed field describes a geometric pattern. Its stability depends on the permitted errors, the norm used to measure them and the property one wants to preserve. Here the property is particularly concrete: within a prescribed spherical tube, the entire zero set must remain one interior C^1 graph over the angular interval. The perturbation is measured only by its values, but belongs to a fixed finite-dimensional band. This restriction allows a positive stability radius; arbitrary smooth errors with small values need not preserve the graph.

Our target is the product of the nine unit-normal mirror forms of B_3, restricted to the unit sphere. We truncate one of its nodal faces before its mirror intersections and work in a closed tube with two normal sides and two angular terminal fibres. Perturbations use all real spherical modes of degree at most nine, without symmetry constraints. A smooth graph is permitted even when the field defining its zero level has a vanishing gradient. This distinction is decisive at the critical radius.

The analysis has three parts. First, the graph-failure radius reduces to a variational cost for a value and an oriented normal derivative. For this target the normal-side escape cost is strictly larger, and the same minimum is obtained by setting both jet components to zero. Second, a moving atomic formula on the sphere gives a sharp lower bound in two geometric regimes, identifies every minimizing point and the unique minimizing field, and proves safety of the entire closed ball. Third, the margin below this radius controls graph position and slope, but an explicit interior approach to the critical field yields unbounded terminal slope despite uniform convergence of the graphs. These are geometric assertions about signed fields; no plate response, particle transport or material deposition is assumed or certified.

1.1 Relation to approximation and discriminant distances

Atomic representations of functionals on finite-dimensional subspaces of $C(K)$ and complementary sign saturation are classical; a useful account is [2, Section 4.2]. That work fixes the sum of the highest-degree coefficients and constructs explicit alternating Chebyshev atoms on diagonally determined sets [2, Theorem 4.8]. For prescribed nodes, [1, Theorem 9] relates exact formulas with ℓ^1 weights to dual ℓ^∞ bounds on sampled data. These principles motivate the certificate here. Its specific ingredients are a moving spherical support for a mixed value–normal-derivative functional, a rational interpolation cancellation on the complete band, and saturation in the continuous tube norm. A single-functional formula does not imply reconstruction of every field from its atoms, nor is a minimal number of atoms asserted.

The complementary fibre bound uses the real trigonometric value–derivative inequality of Erdélyi [3, Theorem 2.1]. We state the imported inequality and check its interval and degree hypotheses in Section 4.2. The remaining finite-dimensional separation, support and rigidity arguments are proved in the article.

Distances to singularity discriminants provide a related viewpoint with different norms and events. Raffalli computes the Bombieri distance for homogeneous forms on the whole sphere and gives a closest contact perturbation at a minimizing point [6, Theorems 5.1 and 5.4]. Kozhasov, Mourrain and Parusiński express higher discriminant distances through Taylor jets in the Bombieri–Weyl geometry [4, Proposition 3.2, equations (3.8)–(3.9)]; their Theorem 5.3 identifies a Chebyshev extremizer among real-rooted binary forms with fixed norm. Our space contains every degree from zero through nine and uses a supremum on a truncated tube. The global B_3 target already has singular mirror intersections. Consequently, the whole-sphere discriminant distance does not supply the positive local radius studied here. The ordinary singularity event uses the value and full tangential gradient; our jet event uses the value and one normal derivative, with escape through the normal sides checked separately.

Lerario and Stecconi obtain isotopy under a strict distance from nontransversality in a differentiable norm and describe the scalar C^1 distance on a closed disk using the value together with the full gradient in the interior and its projection tangent to the boundary on the boundary [5, Lemma 20 and Proposition 31]. Their boundary transversality and isotopy of pairs differ from the fixed-fibre graph property on our tube with angular terminals and corners. In the two exact regimes, the graph at our sharp threshold remains smooth even though the defining level is singular. The comparison identifies the role of the band, norm, domain and preserved property; it does not transfer a conclusion between these settings.

1.2 Organization

Section 2 fixes the problem and states the main results. Sections 3 and 4 reduce graph failure to a jet cost and give general bounds. Section 5 constructs the certificate; Section 6 proves rigidity and the exact regimes. Section 7 gives the two delimiting examples. Sections 8 and 9 treat conditioning and the scope boundaries. Section 10 summarizes the conclusions and the autonomous computational companion. Appendix A justifies the full spherical-band description.

2 Setting and main results

2.1 Target, coordinates, and the closed tube

Let $S^2 = \{(x, y, z) \in \mathbb{R}^3 : x^2 + y^2 + z^2 = 1\}$. On this unit sphere, the target is the product of nine unit-normal linear forms, with multiplicative factor one:

$$f(x, y, z) = \frac{xyz(x^2 - y^2)(x^2 - z^2)(y^2 - z^2)}{8}. \tag{1}$$

This convention does not set the supremum of f to one. The factor $1/8$ is part of the normalization: this is the product of the nine unit-normal linear forms

$$x,\ y,\ z,\quad \frac{x-y}{\sqrt{2}},\ \frac{x+y}{\sqrt{2}},\quad \frac{x-z}{\sqrt{2}},\ \frac{x+z}{\sqrt{2}},\quad \frac{y-z}{\sqrt{2}},\ \frac{y+z}{\sqrt{2}}.$$

We consider the open nodal face $z = 0$, $x > y > 0$ and then truncate it. Fix

$$0 < \eta < \omega < \frac{\pi}{4}, \qquad I = [\eta, \omega], \qquad \delta_\eta = \arctan \frac{\sin \eta \cos \eta}{4}, \qquad a_\eta = \sin \delta_\eta. \tag{2}$$

Dependence on the fixed upper endpoint ω is suppressed in the notation. Define

$$X(\theta, r) = (\cos r \cos \theta, \cos r \sin \theta, \sin r), \qquad D_\eta = I \times [-\delta_\eta, \delta_\eta], \qquad T_\eta = X(D_\eta). \tag{3}$$

Here r is signed geodesic distance from the equator and increases toward positive z. Since $\delta_\eta < \pi/2$ and $0 < \theta < \pi/4$, the chart is injective: its inverse on the tube is $r = \arcsin z$, $\theta = \arctan(y/x)$. Its metric is $dr^2 + \cos^2 r \, d\theta^2$. We distinguish the *normal sides* $r = \pm\delta_\eta$ from the two *angular terminal fibres* $\theta = \eta, \omega$. All four are included in the tube.

2.2 Perturbation class and graph property

We use the full real space

$$\mathcal{V}_9 = \{p|_{S^2} : p \in \mathbb{R}[x, y, z],\ \deg p \le 9\} = \bigoplus_{\ell=0}^{9} \mathcal{H}_\ell(S^2; \mathbb{R}), \qquad \dim \mathcal{V}_9 = 100. \tag{4}$$

Here $\mathcal{H}_\ell$ consists of restrictions of homogeneous harmonic polynomials of degree ℓ. The equality and dimension in (4) are justified in Section 3.2 and Appendix A. There is no symmetry constraint on the perturbation, and it need not lie in the degree-nine eigenspace alone. For $e \in \mathcal{V}_9$, write

$$F = f \circ X, \qquad E = e \circ X, \qquad G_e = F + E, \qquad \|e\|_{T_\eta} = \max_{p \in T_\eta} |e(p)|.$$

The maximum is over the *entire closed tube*; it is not a maximum over sampled points or over a single fibre. This quantity is a norm on $\mathcal{V}_9$ by Lemma 3.4.

Definition 2.1 (The property to be preserved)**.** The property $\mathsf{P}_\eta(e)$ holds if there is a function $h \in C^1(I)$, with $-\delta_\eta < h(\theta) < \delta_\eta$ for every $\theta \in I$, such that

$$\{p \in T_\eta : (f + e)(p) = 0\} = \{X(\theta, h(\theta)) : \theta \in I\}. \tag{5}$$

At the two angular endpoints, C^1 means a continuous one-sided derivative. The definition concerns *all* zeros in T_η and requires strict interiority at the normal sides. It does not require the level set of $f + e$ to be regular.

The failure radius is the infimum

$$\rho_\eta = \inf\{\|e\|_{T_\eta} : e \in \mathcal{V}_9,\ \mathsf{P}_\eta(e) \text{ fails}\}. \tag{6}$$

We introduce the lateral cost and the oriented-jet cost,

$$j_\eta = \min_{\theta \in I} F(\theta, \delta_\eta), \tag{7}$$

$$d_\eta = \inf\left\{ \|e\|_{T_\eta} : \begin{array}{l} e \in \mathcal{V}_9,\ (\theta, r) \in D_\eta, \\ G_e(\theta, r) = 0, \quad \partial_r G_e(\theta, r) \le 0 \end{array} \right\}. \tag{8}$$

Both the field and the point are variables in (8). In particular, the point is not fixed at the centre of a fibre or at an angular endpoint. We initially write an infimum; its attainment is part of the result.

Theorem 2.2 (Finite variational reduction)**.** *For every pair of parameters in* (2)*, j_η and d_η are finite and strictly positive. The infimum defining d_η is a minimum. Moreover,*

$$\boxed{\rho_\eta = \min\{j_\eta, d_\eta\}.} \tag{9}$$

This is an equality of costs. A zero with nonpositive normal derivative is not, by itself, equivalent to failure of Definition 2.1.

Thus the geometric question can be reduced to finitely many field coefficients and a point in a compact two-dimensional domain. The norm constraint remains a condition on a continuum. The theorem neither evaluates d_η in closed form nor substitutes a finite grid for that constraint. Section 3.5 specifies exactly what the reduction does and does not imply at equality.

2.3 General bounds and the exact-radius regimes

Set $a = a_\eta$, $\delta = \delta_\eta$, $L = \omega - \eta$, and define

$$B(\theta) = \frac{\sin^3(2\theta)\cos(2\theta)}{64}, \quad \beta = \min\{B(\eta), B(\omega)\}, \quad A_* = \frac{a\beta}{9}, \quad W(a) = \frac{11a}{10 + a^2}. \tag{10}$$

This B is the normal derivative of the target on the central face, as verified in (15). The Chebyshev polynomial used below is $T_9(t) = \cos(9 \arccos t)$ for $|t| \le 1$, extended polynomially.

Theorem 2.3 (Radius, minimizing fields and the safe threshold)**.** *For every geometry in* (2)*,*

$$\frac{A_*}{2\cos(\delta/2)} \le \rho_\eta = d_\eta \le A_* < j_\eta, \qquad j_\eta \ge \frac{63}{8} A_*. \tag{11}$$

Moreover d_η is also the least norm for the exact jet $G_e = \partial_r G_e = 0$ at a point of the closed tube. Consider either of the following sufficient hypotheses:

Uniform regime L: $\sin(L/4) \ge W(a)$.

Adapted regime M: *there is $\eta < \theta_c < \omega$ such that*

$$\sin((\omega - \theta_c)/2) \ge W(a), \qquad \min\{B(\theta_c), B(\omega)\} \ge 2\cos(\delta/2) B(\eta). \tag{12}$$

Under either hypothesis, $\rho_\eta = d_\eta = A_*$ and the unique field occurring in a minimizing jet pair is

$$e_C(x, y, z) = -A_* T_9(z/a). \tag{13}$$

In L the minimizing points are precisely $(\theta, 0)$ at the angular terminals where $B(\theta) = \beta$, including both terminals in a tie. In M only $(\eta, 0)$ minimizes and $A_* = aB(\eta)/9$. Every field in the closed ball $\|e\|_{T_\eta} \le A_*$ satisfies P_η. The infimum of genuine failures is not attained, whereas γe_C is a genuine failure for every $\gamma > 1$.

The general conclusions follow from Propositions 4.2, 4.4 and 4.5. The exact regimes and threshold assertions are proved in Section 6.2. The two hypotheses are sufficient criteria for the radius formula; neither is asserted to describe the maximal possible geometry. Example 7.1 satisfies M while violating the uniform support condition L. Example 7.2 has $\rho_\eta < A_*$, so a formula valid for every geometry cannot be inferred from these regimes.

2.4 Conditioning before the threshold

The gap to the radius gives quantitative control strictly below the threshold. For a fixed geometry and $\|e\|_{T_\eta} \le m < d_\eta$, Proposition 8.3 gives

$$\partial_r G_e(\theta, h(\theta)) \ge \kappa := \frac{\cos\delta}{2a}(d_\eta - m) > 0, \qquad \|h\|_\infty \le \frac{2m}{\beta}.$$

It also bounds the slope using a finite derivative operator norm on the fixed band and tube. In L or M, $d_\eta = A_*$ is explicit. Theorem 8.5 shows a different phenomenon at equality: fields e_ε strictly inside the ball converge smoothly to e_C, their graphs converge uniformly to zero, yet $|h'_\varepsilon(\theta_*)|$ diverges like $\varepsilon^{-1/3}$ at each minimizing terminal. The critical graph itself is smooth.

3 Variational characterization of graph failure

3.1 Geometry and signs on the whole tube

We first establish the target estimates, including the entire boundary of the tube. Set

$$c = \cos\theta, \quad s = \sin\theta, \quad v = c^2 s^2, \quad C(\theta) = \frac{cs(c^2 - s^2)}{8} > 0, \quad t = \tan r, \quad q = t^2.$$

Substitution into (1), using $c^2 + s^2 = 1$, gives

$$F(\theta, r) = C(\theta)\frac{t(v - q + q^2)}{(1+q)^{9/2}}. \tag{14}$$

In particular, F is odd in r and $F(\theta, 0) = 0$. Define

$$B(\theta) = \partial_r F(\theta, 0) = C(\theta)v = \frac{\cos^3\theta \sin^3\theta \cos 2\theta}{8} > 0. \tag{15}$$

Lemma 3.1 (Positive normal derivative)**.** *On the entire closed rectangle D_η,*

$$\partial_r F(\theta, r) > \frac{B(\theta)}{2} > 0. \tag{16}$$

Consequently $j_\eta > 0$, the unperturbed zero set in the tube is exactly $r = 0$, and $F(\theta, -\delta_\eta) = -F(\theta, \delta_\eta)$.

Proof. Differentiating (14) with $dt/dr = 1 + t^2$, without division by t, yields

$$\partial_r F = C(\theta)\frac{Q(v,q)}{(1+q)^{9/2}}, \qquad Q(v,q) = v - (3+8v)q + 11q^2 - 4q^3. \tag{17}$$

Since $v = \frac{1}{4}\sin^2(2\theta)$ increases on $(0, \pi/4)$,

$$0 \le q \le \tan^2 \delta_\eta = \frac{\sin^2 \eta \cos^2 \eta}{16} \le \frac{v}{16} \le \frac{1}{64}.$$

The inequalities $3 + 8v \le 5$ and $q^2(11 - 4q) \ge 0$ imply $Q(v,q) \ge v - 5q \ge 11v/16$. Also

$$(1+q)^{9/2} \le (65/64)^{9/2} < (65/64)^5 < 11/8,$$

where the last inequality follows from $8 \cdot 65^5 = 9282325000 < 11811160064 = 11 \cdot 64^5$. Combining these bounds proves (16). Oddness was already obtained from (14). Integrating the positive derivative from zero to δ_η gives

$$F(\theta, \delta_\eta) > \tfrac{1}{2}\delta_\eta B(\theta) > 0.$$

Continuity on the compact interval I gives a positive minimum in (7). Strict increase and the zero at $r = 0$ give the remaining claims. □

Corollary 3.2 (Signs below the lateral cost)**.** *If $\|e\|_{T_\eta} < j_\eta$, then, uniformly for $\theta \in I$,*

$$G_e(\theta, -\delta_\eta) < 0 < G_e(\theta, \delta_\eta). \tag{18}$$

Proof. The right-hand value is at least $j_\eta - \|e\|_{T_\eta} > 0$; by oddness of F, the left-hand value is at most $-j_\eta + \|e\|_{T_\eta} < 0$. No symmetry of e is used. □

3.2 The full finite-dimensional space and the minimum of the jet cost

Proposition 3.3 (A complete set of 100 coordinates)**.** *Each $e \in \mathcal{V}_9$ has a unique representation on the sphere of the form*

$$e(x,y,z) = A(y,z) + xB(y,z), \qquad \deg A \le 9, \quad \deg B \le 8. \tag{19}$$

The corresponding 55 monomials of A and 45 monomials of B form a basis of $\mathcal{V}_9$.

Proof. In any ambient polynomial of degree at most nine, repeatedly replace x^2 by $1 - y^2 - z^2$. This preserves its restriction to the sphere, does not increase degree, and produces (19). For uniqueness, suppose the expression in (19) vanishes on the sphere. At every point with $y^2 + z^2 < 1$, evaluate it at the two values $x = \pm\sqrt{1 - y^2 - z^2}$. Adding and subtracting gives $A(y,z) = B(y,z) = 0$ on the open disk. A polynomial vanishing on an open set is identically zero: one may fix one coordinate on a small rectangle and apply the one-variable zero theorem successively to its coefficients. Thus all coefficients vanish. There are $(9+1)(9+2)/2 = 55$ monomials of degree at most nine in two variables and $(8+1)(8+2)/2 = 45$ of degree at most eight. □

Lemma 3.4 (The tube norm and compact sublevels)**.** *For fixed parameters* (2)*, $\|\cdot\|_{T_\eta}$ is a norm on $\mathcal{V}_9$, and every set $\{e : \|e\|_{T_\eta} \le M\}$ with $M < \infty$ is compact in coefficient coordinates.*

Proof. Only positive definiteness needs proof. The tube contains a nonempty open subset U of the sphere. If e vanishes on T_η, it vanishes on U. Its restriction to a great circle is a trigonometric polynomial of degree at most nine: each ambient coordinate is linear in the sine and cosine of the circle parameter. Such a polynomial that vanishes on an open arc vanishes on the whole circle, since multiplication by $\exp(9it)$ makes it an ordinary polynomial in $\exp(it)$ with infinitely many roots. For any $q \in S^2$, choose a point of U not parallel to q and the great circle through them. That circle contains an open arc in U, so $e(q) = 0$. Hence e is the zero function on the sphere.

For compactness, let $b_1, \dots, b_{100}$ be the basis from Proposition 3.3. Evaluations at points of T_η span the dual of $\mathcal{V}_9$. Otherwise a nonzero field would be annihilated by every such evaluation, contradicting positive definiteness. Select 100 linearly independent evaluations. The matrix $M_{ij} = b_j(p_i)$ is invertible, and $\|e\|_{T_\eta} \le M_0$ bounds every coordinate of $(e(p_i))_{i=1}^{100}$ by M_0. It therefore bounds the coefficient vector by application of M^{-1}. Finally,

$$\big|\|e_c\|_{T_\eta} - \|e_{c'}\|_{T_\eta}\big| \le \|e_c - e_{c'}\|_{T_\eta} \le \sum_{j=1}^{100} |c_j - c'_j| \; \|b_j\|_{T_\eta} \,,$$

so the sublevel set is closed. The result follows from compactness of closed bounded sets in $\mathbb{R}^{100}$. □

The evaluation points above are a compactness argument, not a numerical norming mesh or an algorithm for computing the sup. The bound on the inverse matrix may depend on η and ω; no uniform bound as the tube degenerates is asserted.

Proposition 3.5 (Attainment of the oriented-jet cost)**.** *The infimum in* (8) *is attained by some pair* $(e_*, (\theta_*, r_*))$*, and* $d_\eta > 0$*.*

Proof. The feasible set is nonempty: $e = -f \in \mathcal{V}_9$ makes G_e and $\partial_r G_e$ identically zero. Set $M_0 = \|f\|_{T_\eta}$. It suffices to minimize over pairs in

$$\{e \in \mathcal{V}_9 : \|e\|_{T_\eta} \le M_0\} \times D_\eta$$

satisfying the two jet conditions. This product is compact by Lemma 3.4. The conditions $G_e = 0$ and $\partial_r G_e \le 0$ are closed, because value and derivative depend continuously on coefficients and point. The norm is continuous, so it attains a minimum on this nonempty closed subset. Candidates of norm larger than M_0 cannot improve it, as the candidate $-f$ already has norm M_0. If the minimum were zero, positive definiteness would force $e_* = 0$. But $\partial_r F > 0$ everywhere on D_η, which is incompatible with the derivative constraint. Thus the minimum is strictly positive. □

3.3 From oriented fibre zeros to a C^1 graph

Injectivity of X implies that one interior zero on each fibre gives a set-theoretic graph. It also gives a continuous graph in this setting: if $\theta_n \to \theta$, any subsequential limit of the roots lies in $[-\delta_\eta, \delta_\eta]$, is a root at θ by continuity, and must equal its unique root. This compactness argument does not supply a derivative. The stronger hypothesis below supplies it, without assuming that G_e is monotone away from its zeros.

Lemma 3.6 (Fibre-to-graph lemma)**.** *Suppose* (18) *holds and*

$$G_e(\theta, r) = 0 \quad \Longrightarrow \quad \partial_r G_e(\theta, r) > 0 \qquad ((\theta, r) \in D_\eta). \tag{20}$$

Then $\mathsf{P}_\eta(e)$ *holds, including both angular terminal fibres.*

Proof. Fix θ. The side signs give an interior zero by the intermediate value theorem. Every zero is simple by (20), hence isolated. The zero set of this fibre is compact and is disjoint from the normal endpoints. It is finite: an infinite set would have an accumulation point that is also a zero, contradicting simplicity there. Every zero crosses from negative to positive as r increases. If two consecutive zeros existed, the function would be positive just after the first and negative just before the second; continuity would give another zero between them. This contradicts consecutiveness. Thus there is exactly one zero, denoted $h(\theta)$.

For completeness, the local scalar implicit-function argument can be made directly. At a zero (θ_0, r_0), continuity of the derivative gives a small open rectangle on which $\partial_r G_e$ is bounded below by a positive number. At θ_0 choose two nearby normal values around r_0 with opposite signs. Those signs persist on a smaller open interval of θ values. The intermediate value theorem and strict monotonicity on that rectangle give a unique local root. The preceding compactness argument gives its continuity. Applying the mean value theorem separately in the two variables to

$$G_e(\theta + t, h(\theta + t)) - G_e(\theta, h(\theta)) = 0$$

and letting $t \to 0$ then gives

$$h'(\theta) = -\frac{\partial_\theta G_e(\theta, h(\theta))}{\partial_r G_e(\theta, h(\theta))}. \tag{21}$$

The denominator stays positive locally, so this derivative is continuous. Their restrictions to I agree wherever they overlap, by fibrewise uniqueness.

The same argument applies at $\theta = \eta$ and $\theta = \omega$: the field is a global polynomial restriction and the chart is defined on an open neighbourhood of the closed rectangle. Apply the local argument there and then restrict to I. This supplies the required one-sided endpoint derivatives. The side signs exclude zeros on $r = \pm\delta_\eta$, and fibrewise uniqueness accounts for all zeros in the tube. □

Corollary 3.7 (A necessary event below j_η)**.** *If $\|e\|_{T_\eta} < j_\eta$ and $\mathsf{P}_\eta(e)$ fails, there is a point of D_η at which $G_e = 0$ and $\partial_r G_e \le 0$.*

Proof. Corollary 3.2 gives the side signs. The conclusion is the contrapositive of Lemma 3.6. □

Example 3.8 (A singular level with a smooth graph)**.** The field $e = -f + z^3$ belongs to $\mathcal{V}_9$ and gives $G_e(\theta, r) = \sin^3 r$. Its entire zero set in T_η is the smooth graph $r = 0$, while $\partial_r G_e = 0$ at every zero; indeed the spherical gradient of $f + e = z^3$ vanishes there. This example shows why the jet condition is not a pointwise characterization of failure. It is not being asserted to have norm below j_η, to minimize d_η, or to identify an equality case of the sharp radius.

3.4 Proof of the reduction

The existence and positivity assertions of Theorem 2.2 follow from Lemma 3.1 and Proposition 3.5. We prove the two inequalities for (9) separately.

3.4.1 Every failure costs at least $\min(j_\eta, d_\eta)$

Let e violate P_η. If $\|e\|_{T_\eta} \ge j_\eta$, the desired lower bound is immediate. Otherwise Corollary 3.7 provides a point satisfying the two jet constraints, so $\|e\|_{T_\eta} \ge d_\eta$ by definition.

Taking the infimum over genuine failures gives

$$\rho_\eta \geq \min\{j_\eta, d_\eta\}. \tag{22}$$

3.4.2 A genuine failure at the lateral cost

Let $\theta_j \in I$ minimize $F(\theta, \delta_\eta)$. The constant field $e = -j_\eta$ belongs to $\mathcal{V}_0 \subset \mathcal{V}_9$, has norm j_η, and produces

$$G_e(\theta_j, \delta_\eta) = 0.$$

This zero on a normal side violates strict interiority in Definition 2.1. Hence

$$\rho_\eta \leq j_\eta. \tag{23}$$

We have not assumed that the minimum occurs at $\theta = \eta$.

3.4.3 Approaching the jet cost by genuine failures

It remains to consider $d_\eta < j_\eta$. Choose a minimizing pair $(e_*, (\theta_*, r_*))$ from Proposition 3.5. It satisfies $|r_*| < \delta_\eta$: a zero on either normal side would require

$$|e_*(X(\theta_*, r_*))| = |F(\theta_*, r_*)| \geq j_\eta > d_\eta,$$

which is impossible. Put $z_* = \sin r_*$ and, for $\varepsilon > 0$, define the global field

$$e_\varepsilon(x, y, z) = e_*(x, y, z) - \varepsilon(z - z_*). \tag{24}$$

The correction is in $\mathcal{V}_1 = \mathcal{H}_0 \oplus \mathcal{H}_1$ and so remains in the original admissible space. At the selected point,

$$G_{e_\varepsilon}(\theta_*, r_*) = 0, \qquad \partial_r G_{e_\varepsilon}(\theta_*, r_*) = \partial_r G_{e_*}(\theta_*, r_*) - \varepsilon \cos r_* < 0. \tag{25}$$

The value is unchanged, and $\cos r_* > 0$ on this tube. On the *whole tube*, $|z| \leq a_\eta$ and $|z_*| < a_\eta$, so

$$\|e_\varepsilon\|_{T_\eta} \leq d_\eta + \varepsilon(a_\eta + |z_*|) \leq d_\eta + 2a_\eta\varepsilon. \tag{26}$$

Choose

$$0 < \varepsilon < \frac{j_\eta - d_\eta}{2a_\eta}. \tag{27}$$

The field e_ε still has the strict side signs (18). By the negative derivative in (25), there is a small $s > 0$ for which

$$-\delta_\eta < r_* - s < r_* < r_* + s < \delta_\eta, \qquad G_{e_\varepsilon}(\theta_*, r_* - s) > 0, \quad G_{e_\varepsilon}(\theta_*, r_* + s) < 0.$$

Together with the negative sign at $-\delta_\eta$ and positive sign at δ_η, the intermediate value theorem gives one zero in $(-\delta_\eta, r_* - s)$ and another in $(r_* + s, \delta_\eta)$. Along with r_*, these are three distinct interior zeros on the same fibre. Thus $\mathsf{P}_\eta(e_\varepsilon)$ genuinely fails. The argument is unchanged if θ_* is either angular endpoint, since that entire fibre is included in D_η.

Letting $\varepsilon \downarrow 0$ in (26) yields $\rho_\eta \leq d_\eta$. If instead $d_\eta \geq j_\eta$, the lateral witness already suffices. Combining these facts with (22) proves Theorem 2.2. In particular, the proof never replaces an admissible global field by a freely chosen one-variable perturbation of a single fibre.

3.5 Equality, attainment, and the limits of the conclusion

Proposition 3.9 (What happens at the threshold)**.** *The reduction has the following consequences.*

1. *Every field of norm strictly less than ρ_η satisfies P_η.*
2. *If $j_\eta \le d_\eta$, the constant field $-j_\eta$ realizes a genuine failure of norm $\rho_\eta = j_\eta$.*
3. *If $d_\eta < j_\eta$, the closed ball $\{e : \|e\|_{T_\eta} \le d_\eta\}$ is safe if and only if every field that occurs in a minimizing pair for the jet problem satisfies P_η. In the same case, the infimum of genuine failures is attained if and only if some jet-minimizing field violates P_η.*

Proof. The first assertion is the defining property of an infimum, and the second follows from the lateral witness. For the third, any failure of norm at most d_η is below j_η and therefore has a feasible jet by Corollary 3.7. Its norm is at least d_η by definition, so it equals d_η and occurs in a minimizing pair. Conversely, a jet-minimizing field that violates P_η is a failure of precisely that norm. These two implications prove both equivalences. □

This case distinction records the logic of the reduction. Proposition 4.4 proves that only $d_\eta < j_\eta$ occurs in the present family. The classification in Section 6.2 then identifies a safe jet minimizer in the exact regimes. Correction (24) gives unsafe fields converging to it in the same tube norm.

The distinction is substantive. The jet feasible set is closed and has a minimizing pair. Definition 2.1 allows singular levels, so those facts alone do not make the failure set closed, do not settle the closed-ball threshold, and do not provide a uniform C^1 conditioning bound for the graph. Example 3.8 separates geometric regularity of the graph from regularity of the defining level.

Mathematical and physical boundaries. The result is for real fields, the complete degree-at-most-nine space, the stated normalization, and one closed truncated tube. It makes no claim about the global nodal topology, vertices outside the tube, arbitrary out-of-band errors, complex phasor zeros, modulus or RMS zeros, material deposition, or the realization of every admissible perturbation by a particular apparatus. No numerical search or physical experiment is used in this proof. Finite dimensionality supplies compactness but leaves the continuous sup constraint intact.

Route to the sharp result. The next sections prove the dual description, the complementary lower bounds and central rigidity. They then classify the minimizing pairs and prove closed-ball safety in the two exact regimes, followed by the two examples. The quantitative graph bounds and their critical limit are treated in Section 8.

4 Dual jet costs and tube-wide bounds

4.1 Pointwise jet costs and their dual description

For the rest of the text abbreviate $a = a_\eta$, $\delta = \delta_\eta$ and $L = \omega - \eta$. At $p = (\theta, r) \in D_\eta$, let $v_p(e) = E(\theta, r)$ and $\ell_p(e) = E_r(\theta, r)$. The pointwise cost is

$$D(p) = \min\{\|e\|_{T_\eta} : e \in \mathcal{V}_9,\ v_p(e) = -F(p),\ \ell_p(e) \le -F_r(p)\}. \tag{28}$$

The field $-f$ is feasible. The compactness argument of Proposition 3.5 applies with p fixed, so this minimum exists and is positive. The joint minimizing pair in that proposition gives

$d_\eta = \min_{p\in D_\eta} D(p)$; no regularity assertion about the function D is needed for this equality. Neither constraint in (28) is removed by any symmetry projection.

For a real linear functional h on $\mathcal{V}_9$, put $\|h\|_* = \max_{\|e\|_{T_\eta}\le 1} |h(e)|$. This dual norm uses the whole tube. A pair $\lambda \in \mathbb{R}$, $\mu \ge 0$ with $\|\lambda v_p + \mu \ell_p\|_* \le 1$ gives

$$\|e\|_{T_\eta} \ge -(\lambda v_p + \mu \ell_p)(e) \ge \lambda F(p) + \mu F_r(p) \tag{29}$$

for every feasible field. In particular a multiplier of value equal to zero does not remove the value constraint from the primal problem.

Proposition 4.1 (Exact pointwise duality)**.** *At every $p \in D_\eta$,*

$$D(p) = \max_{\lambda\in\mathbb{R},\ \mu\ge 0} \{\lambda F(p) + \mu F_r(p) : \|\lambda v_p + \mu \ell_p\|_* \le 1\}. \tag{30}$$

Both extrema are attained. For any optimal primal field and dual pair,

$$\mu\big(\ell_p(e) + F_r(p)\big) = 0, \qquad -(\lambda v_p + \mu \ell_p)(e) = \|e\|_{T_\eta} = D(p).$$

Proof. We give the finite-dimensional separation argument directly. The image C of the unit ball under $e \mapsto (v_p(e), \ell_p(e))$ is compact, convex and symmetric. It contains zero in its interior: the fields 1 and $z - \sin r$ have independent images $(1, 0)$ and $(0, \cos r)$, with $\cos r > 0$. For $0 < s < D(p)$, the compact set sC and the closed half-line $H = \{(-F(p), w) : w \le -F_r(p)\}$ are disjoint. Their distance is positive and attained. The line orthogonal to the difference of a closest pair strictly separates them, by the usual first-variation inequalities for distance on convex sets.

Write the separating functional, oriented with its larger values on H, as $\varphi(v, w) = -\lambda v - \mu w$. Its infimum on H is finite only when $\mu \ge 0$. Normalize by $\max_C \varphi = \|\lambda v_p + \mu \ell_p\|_* = 1$, which is positive because C contains zero in its interior. Strict separation gives $\lambda F(p) + \mu F_r(p) > s$. The feasible multiplier set is compact: the linear map $(\lambda, \mu) \mapsto \lambda v_p + \mu \ell_p$ is injective, so its dual norm bounds the two coefficients. Letting $s \uparrow D(p)$ and taking a convergent subsequence proves the reverse inequality to (29) and attainment of the maximum. The two inequalities in (29) must then both be equalities, giving the displayed conclusions. □

An exact norm for a constructed functional need not make its objective the maximum in (30). The certificates below therefore give lower bounds, except at the central points where a feasible field also attains the bound.

4.1.1 Exact and oriented jets

Proposition 4.2 (Active derivatives and normal-side costs)**.** *If $|r| < \delta$, then $D(\theta, r) > |F(\theta, r)|$. Every optimal dual pair in* (30) *has $\mu > 0$, and every optimal primal field has $E_r = -F_r$. At either normal side, $D(\theta, \pm\delta) = |F(\theta, \pm\delta)|$. There an optimal field with $E_r = -F_r$ exists, although other optimal fields have $E_r < -F_r$ and every optimal oriented-dual pair has $\mu = 0$. Consequently, on the entire closed tube,*

$$D(p) = \min\{\|e\|_{T_\eta} : e \in \mathcal{V}_9,\ G_e(p) = 0,\ \partial_r G_e(p) = 0\}. \tag{31}$$

Proof. At an interior normal point, a feasible field of norm $|F(p)|$ would attain a maximum of its absolute value along the fibre there, so $E_r(p) = 0$, contradicting $E_r(p) \le -F_r(p) < 0$. If $F(p) = 0$, norm zero would force $e = 0$, with the same contradiction. Since $\|v_p\|_* = 1$ (constant fields attain this value), a dual optimum with $\mu = 0$ could achieve at most

$|F(p)|$. Thus $\mu > 0$, and Proposition 4.1 gives the derivative equality for every primal optimum. These arguments include angular terminals: only interiority along the normal coordinate is used.

For the sides use the exact target factors derived in Section 4.2, equation (32):

$$R_\theta(q) = (1-q)^4 - \frac{q(1-q)^2(1-2q)}{v_\theta}, \qquad S_\theta = R_\theta + 2qR'_\theta.$$

The derivative of $q(1-q)^2(1-2q)$ is $(1-q)(1-7q+8q^2) > 0$ for $0 \le q \le a^2 < 1/65$. Hence $R'_\theta < 0$ and (33) gives $0 < S_\theta(a^2) < R_\theta(a^2)$. For either $p = (\theta, \pm\delta)$ the global linear field

$$e_{\mathrm{lin}} = -F(\theta,\delta)\frac{z}{a}$$

has value $-F(p)$, norm $|F(p)|$ and normal derivative $-B(\theta)\cos\delta\, R_\theta(a^2) < -F_r(p)$. The opposite bound follows from the value constraint. With $\kappa = S_\theta(a^2)/R_\theta(a^2) \in (0,1)$, the field

$$e_{\mathrm{eq}} = \kappa e_{\mathrm{lin}} + (1-\kappa)(-F(p))$$

mixes this linear field with a constant. It retains the prescribed value, has the exact normal derivative, and has norm at most $|F(p)|$ by convexity, hence exactly $|F(p)|$. Complementarity with the strict linear optimum forces $\mu = 0$ for every optimal oriented-dual pair. This proves equality of the two minimum values, not equality of their sets of minimizers at the normal sides. □

4.2 Target estimates and a complementary fibre barrier

4.2.1 Uniform target bounds on the original domain

Write $v_\theta = \sin^2\theta\cos^2\theta$, as in Section 3.1, and introduce the normalized normal coordinate $t = \sin r/a$. The identity

$$a^2 = \frac{v_\eta}{16+v_\eta} < \frac{1}{65}, \qquad \frac{a^2}{v_\theta} < \frac{1}{16}$$

holds throughout the original angular interval. Direct substitution of $z = \sin r$ into (1) gives

$$\begin{aligned} F(\theta, \arcsin z) &= B(\theta) z R_\theta(z^2), \qquad F_r(\theta, \arcsin z) = B(\theta)\sqrt{1-z^2}\, S_\theta(z^2), \\ R_\theta(q) &= 1 - c_1 q + c_2 q^2 - c_3 q^3 + c_4 q^4, \qquad S_\theta(q) = R_\theta(q) + 2qR'_\theta(q), \\ (c_1,c_2,c_3,c_4) &= (4 + 1/v_\theta,\ 6 + 4/v_\theta,\ 4 + 5/v_\theta,\ 1 + 2/v_\theta). \end{aligned} \tag{32}$$

For example the unsimplified factor is $(1-q)^2[(1-q)^2 - q(1-q)/v_\theta + q^2/v_\theta]$, which expands to R_θ. Here $B(\theta)$ is the positive quantity in (15). These are exact identities, not a truncation of the target.

For $0 \le q \le a^2$, both remainders after the linear terms are nonnegative, since

$$c_2 - c_3 q + c_4 q^2 \ge 6 + 4/v_\theta - (4 + 5/v_\theta)/65 > 0,$$

$$5c_2 - 7c_3 q + 9c_4 q^2 \ge 30 + 20/v_\theta - (28 + 35/v_\theta)/65 > 0.$$

Moreover $c_1 a^2 < 4/65 + 1/16 = 129/1040 < 1/8$. Consequently

$$R_\theta(a^2t^2) \ge 1 - t^2/8, \qquad S_\theta(a^2t^2) \ge 1 - 3t^2/8 > 0 \quad (|t| \le 1). \tag{33}$$

These estimates require no extra small-angle assumption or restriction on perturbation coefficients. Put

$$A_\theta = \frac{aB(\theta)}{9}. \tag{34}$$

4.2.2 A trigonometric inequality and its application

For a real trigonometric polynomial Q of degree at most a positive integer n, and $0 < d < \pi$, Erdélyi's Theorem 2.1 gives, for $|r| < d$,

$$|Q'(r)|^2 + \beta_{n,d}(r)^2|Q(r)|^2 \le \beta_{n,d}(r)^2 \max_{|s|\le d}|Q(s)|^2, \qquad \beta_{n,d}(r) = \frac{n\cos(r/2)}{\sqrt{\sin^2(d/2) - \sin^2(r/2)}}. \tag{35}$$

We use the author's 18-page manuscript [3, Theorem 2.1, pp. 4–5; proof, pp. 9–11]. Its width parameter is d, distinct from our oriented-jet cost d_η.

For fixed θ, every ambient monomial of degree at most nine restricts to a trigonometric polynomial in r of degree at most nine. Thus (35) applies to $E(\theta,\cdot)$ with $n = 9$ and $d = \delta$. Its fibre supremum is at most $\|e\|_{T_\eta}$. At a feasible jet, $E = -F$ and $|E_r| \ge F_r > 0$, giving

$$D(\theta,r) \ge K(\theta,r) := \sqrt{F(\theta,r)^2 + F_r(\theta,r)^2/\beta_{9,\delta}(r)^2} \quad (|r| < \delta). \tag{36}$$

At $r = \pm\delta$ use instead $D \ge |F|$, from the value constraint. Defining $K = |F|$ there makes this bound continuous. In particular $K(\theta,0) = A_\theta/[2\cos(\delta/2)] < A_\theta$: this fibre bound alone does not give the central value of D.

Proposition 4.3 (Uniform complementary barrier)**.** *For every point of the closed tube, with $u = t^2$,*

$$\frac{D(\theta,r)^2}{A_\theta^2} \ge \mathcal{Q}(u) := 81u(1-u/8)^2 + \frac{16}{65}(1-u)(1-3u/8)^2. \tag{37}$$

Consequently

$$D(\theta,r) \ge \frac{4}{\sqrt{65}}A_\theta \quad \textit{everywhere}, \qquad D(\theta,r) > A_\theta \quad \textit{if } |t| \ge 1/10. \tag{38}$$

Proof. Set $c = \sqrt{1-a^2u}$ and $c_\delta = \cos\delta$. In the interior,

$$\frac{c^2}{a^2}\frac{\sin^2(\delta/2) - \sin^2(r/2)}{\cos^2(r/2)} = \frac{c^2(1-u)}{(1+c)(c+c_\delta)} \ge \frac{16}{65}(1-u),$$

because $c^2 \ge c_\delta^2 > 64/65$ and the denominator is at most 4. Equations (32)–(36) give (37). At the normal sides $u = 1$, its second term is zero and the separate value bound gives the same conclusion.

On $[0,1]$ the first summand of $\mathcal{Q}$ has derivative $81(1-u/8)(1-3u/8) \ge 2835/64$. The derivative of the second is bounded below by $-(16/65)(1+3/4) = -28/65$. Hence $\mathcal{Q}' > 0$, and $\mathcal{Q}(0) = 16/65$. Also

$$\mathcal{Q}(1/100) > \frac{81}{100}\left(\frac{99}{100}\right)^2 + \frac{16}{65}\left(\frac{99}{100}\right)^3 = \frac{67127049}{65000000} > 1.$$

These facts prove both assertions, including the angular terminals and the normal sides. □

4.2.3 The universal radius and a sharper floor

The function B has derivative

$$B'(\theta) = \frac{\sin^2(2\theta)}{32}(3 - 4\sin^2(2\theta)). \tag{39}$$

It increases strictly up to $\pi/6$ and decreases strictly afterwards. Thus $B \geq \beta$ on I, and its minimum is reached only at those endpoints which realize β.

Proposition 4.4 (The normal-side event is never first)**.** *On the whole original domain, $\rho_\eta = d_\eta \leq A_* < j_\eta$ and $j_\eta \geq 63A_*/8$. Every minimizing jet pair is interior in the normal coordinate.*

Proof. The field e_C in (13) has norm A_* and at each $(\theta_*, 0)$ with $B(\theta_*) = \beta$ satisfies $E_C = -F = 0$ and $(E_C)_r = -9A_*/a = -F_r$. Therefore $d_\eta \leq A_*$. At $r = \delta$, (33) gives $F(\theta, \delta) \geq 7aB(\theta)/8$. Minimizing in θ gives $j_\eta \geq 63A_*/8 > A_*$. Theorem 2.2 proves the assertion about ρ_η. A point on a normal side costs at least j_η by its value constraint, so cannot occur in a minimizing pair. □

Proposition 4.5 (A stronger all-point floor)**.** *Put $g = [2(1 + \cos\delta)]^{-1}$. For every point of the closed tube,*

$$\frac{D(\theta, r)^2}{A_\theta^2} \geq g + 61t^2, \qquad D(\theta, r) \geq \frac{A_\theta}{2\cos(\delta/2)}. \tag{40}$$

The second inequality is strict when $r \neq 0$. In particular $A_*/[2\cos(\delta/2)] \leq \rho_\eta \leq A_*$.

Proof. For $u = t^2$ and $c = \sqrt{1 - a^2u}$, keep the exact derivative factor from the preceding proof instead of replacing it by a constant:

$$\frac{c^2(1-u)}{(1+c)(c+\cos\delta)} \geq g(1 - a^2u)(1 - u).$$

The denominator is at most $2(1 + \cos\delta)$. Applying the target bounds gives

$$\frac{D^2}{A_\theta^2} \geq 81u(1 - u/8)^2 + g(1 - a^2u)(1 - u)(1 - 3u/8)^2.$$

At $u = 1$ the derivative term is zero and the value constraint gives the same inequality. Since $(1 - u/8)^2 \geq 49/64$ and $\prod_i(1 - x_i) \geq 1 - \sum_i x_i$ for $x_i \in [0, 1]$, the last display is at least

$$g + \left(\frac{3969}{64} - g(a^2 + 7/4)\right) u \geq g + 61u.$$

Indeed $g < 1/2$ and $a^2 + 7/4 < 2$ make the coefficient greater than 61. Finally $\sqrt{g} = 1/[2\cos(\delta/2)]$ and $A_\theta \geq A_*$, while Proposition 4.4 supplies the upper bound and the identity of costs. □

Corollary 4.6 (Localization and reflection of minimizing points)**.** *Every minimizing pair has $|t| < 1/10$ and $B(\theta) \leq 2\cos(\delta/2)\beta$, with the latter inequality strict if $t \neq 0$. Moreover $D(\theta, -r) = D(\theta, r)$.*

Proof. The outer bound (38) and $d_\eta \leq A_*$ exclude $|t| \geq 1/10$. The sharper floor gives the angular restriction. The transformation $e(x, y, z) \mapsto -e(x, y, -z)$ preserves the space and tube norm. At the reflected point it reverses the value and preserves the normal derivative, exactly as required by the oddness of F and evenness of F_r. Applying it twice proves the equality of costs. □

In particular the sharper all-point floor complements, rather than replaces, the $\mathcal{Q}$ barrier needed at $|t| = 1/10$.

5 The spherical atomic certificate

5.1 An atomic certificate on all 100 modes

The existence of a norm-preserving atomic formula for a functional on a finite-dimensional subspace of $C(K)$, and the extremal sign conditions at its atoms, are classical [2, Theorem 4.4, Corollary 4.5 and Proposition 4.7]. At prescribed nodes, the relation between exact formulas and minimal weight norms is described by [1, Section 3, Theorem 9]. Representing one functional does not reconstruct every field from those evaluations. Here the work is to exhibit supported points and weights, prove the identity on the complete spherical space and attain the continuous tube norm explicitly.

5.1.1 A common geometric condition

Fix $\tau = 1/10$ and $r_t = \arcsin(at)$, $c_t = \sqrt{1-a^2t^2}$. At an angular position θ, choose a nonzero signed angle α such that the closed segment between θ and $\theta+\alpha$ lies in I. Assume

$$\sin(|\alpha|/2) \geq W(a), \qquad W(a) = \frac{11a}{10+a^2}. \tag{41}$$

In particular $|\alpha| \leq L < \pi/4$. For each fixed θ, t, α, with $|t| \leq \tau$, define

$$\begin{gathered} w = e^{i\alpha} - 1, \quad h = |w|^2 = 4\sin^2(\alpha/2), \\ b_t(s) = \frac{1-a^2ts}{c_t}, \quad q_t(s) = \frac{a^2(s-t)^2}{c_t^2 h} \quad (-1 \leq s \leq 1). \end{gathered} \tag{42}$$

All derivatives in s below hold θ, t, α fixed. In particular they do not differentiate a choice of angular side with respect to its centre. The positive affine function b_t is tangent to $c(s) = \sqrt{1-a^2s^2}$ at $s = t$:

$$b_t(t) = c_t, \quad b_t'(t) = c'(t) = -a^2t/c_t, \quad b_t(s)^2 - c(s)^2 = \frac{a^2(s-t)^2}{c_t^2}. \tag{43}$$

The following exact maximum determines reality of the intersections:

$$\max_{|s|\leq 1,\ |t|\leq\tau} \frac{a|s-t|}{1-a^2ts} = W(a). \tag{44}$$

Indeed, for fixed t, the quotient without absolute value has derivative $(1-a^2t^2)/(1-a^2ts)^2 > 0$ with respect to s. The maximum of the absolute value is at $s = \pm 1$. For $t \geq 0$, the difference between the two endpoint ratios, after removing a, is $2t(1-a^2)/(1-a^4t^2) \geq 0$, selecting $s = -1$. By reflection, the maximum at fixed t is $a(1+|t|)/(1+a^2|t|)$, strictly increasing in $|t|$. Equality in (44) occurs only at $(s,t) = (-1,\tau), (1,-\tau)$.

5.1.2 Points in the tube and conditional weights

Let

$$S_\pm(s) = \frac{b_t(s) \pm \sqrt{b_t(s)^2 - 4q_t(s)}}{2}. \tag{45}$$

Equations (41) and (44) imply that these are real and belong to $[0, b_t(s)]$, since

$$\frac{4q_t(s)}{b_t(s)^2} = \frac{1}{\sin^2(\alpha/2)} \left(\frac{a|s-t|}{1-a^2ts}\right)^2 \leq 1.$$

Use rotated coordinates $u = x\cos\theta + y\sin\theta$, $v = -x\sin\theta + y\cos\theta$ and define points $Q_{s,\pm}$ by

$$u + iv = b_t(s) + S_\pm(s)w, \qquad z = as. \tag{46}$$

The quadratic equation for S and (43) give $|u+iv|^2 = 1 - a^2s^2$. Thus these are points on the original sphere. For $0 \le \xi \le 1$ the argument of $1 + \xi(e^{i\alpha} - 1)$ lies between 0 and α: its real part is positive and

$$\frac{\mathrm{Im}}{\mathrm{Re}} = \frac{\xi\sin\alpha}{1 - \xi + \xi\cos\alpha}$$

is monotone with the sign of α. Taking $\xi = S_\pm/b_t$ proves $Q_{s,\pm} \in T_\eta$, even when θ is a terminal. The auxiliary endpoints b_t and $b_t e^{i\alpha}$ themselves need not lie on the sphere.

Define the probability measure

$$\pi_{t,s} = \frac{S_+(s)}{b_t(s)}\delta_{Q_{s,-}} + \frac{S_-(s)}{b_t(s)}\delta_{Q_{s,+}}. \tag{47}$$

At $s = t$, the roots are 0 and $b_t(t)$, so the weights are 1 and 0. For $s \neq t$ both weights are positive. At a repeated root the two half-weights are added at their common point.

5.1.3 Moment recurrence and both data of the jet

For the distribution on the coordinate S underlying (47), its moments satisfy

$$m_0 = 1, \quad m_1 = 2q_t/b_t, \qquad m_n = b_t m_{n-1} - q_t m_{n-2} \quad (n \ge 2). \tag{48}$$

This follows from $S^2 - b_t S + q_t = 0$ and remains true at repeated roots. Set $k_n = b_t m_n$. Then

$$k_0 = b_t, \quad k_1 = 2q_t, \quad k_n = b_t k_{n-1} - q_t k_{n-2}, \qquad \deg_s k_n \le n + 1.$$

The degree bound follows by induction from $\deg b_t \le 1$ and $\deg q_t \le 2$. Hence

$$\begin{aligned} R_m(t,s) := \int (u+iv)^m \, d\pi_{t,s} &= \sum_{n=0}^{m} \binom{m}{n} b_t(s)^{m-n} w^n m_n(s) \\ &= \frac{P_{m+1}(s)}{b_t(s)}, \qquad \deg P_{m+1} \le m+1. \end{aligned} \tag{49}$$

Because $q_t(t) = q_t'(t) = 0$, (48) also gives $m_n(t) = m_n'(t) = 0$ for $n \ge 1$. Thus

$$R_m(t,t) = c_t^m, \qquad \partial_s R_m(t,t) = m c_t^{m-1} c'(t). \tag{50}$$

For completeness, the real and imaginary parts of

$$z^k(u+iv)^m, \qquad k + m \le 9, \tag{51}$$

with only the real part when $m = 0$, form a basis of $\mathcal{V}_9$. There are $10+2(9+8+\cdots+1) = 100$ such functions. They are independent: at fixed $z \in (-1,1)$, put $u + iv = \sqrt{1-z^2}e^{i\phi}$. Fourier uniqueness in ϕ forces each polynomial coefficient in z to vanish; its nonzero spherical factor $(1-z^2)^{m/2}$ can be divided out. Varying z shows that all coefficients vanish. Proposition 3.3 supplies the dimension, so independence proves completeness.

For every real field $e \in \mathcal{V}_9$, equations (49)–(50) imply

$$g_e(s) := \int e \, d\pi_{t,s} = \frac{P_e(s)}{b_t(s)}, \quad \deg P_e \le 10, \qquad g_e(t) = E(\theta, r_t), \quad g_e'(t) = \frac{a}{c_t} E_r(\theta, r_t). \tag{52}$$

The factor $z^k = a^k s^k$ contributes its ordinary product-rule derivative, so the statement includes every k, m in (51). This reproduces the two original jet data. It does not assert that an arbitrary field or its average is a free polynomial of degree nine. The degree-ten numerator is retained and handled next.

5.1.4 Rational interpolation and signs

Let $P = T_9$ and $U = U_8$, with their explicit forms

$$\begin{aligned} P(s) &= 9s - 120s^3 + 432s^5 - 576s^7 + 256s^9, \\ U(s) &= 1 - 40s^2 + 240s^4 - 448s^6 + 256s^8, \qquad P' = 9U, \\ N(s) &= (s^2 - 1)U(s), \qquad s_j = \cos(j\pi/9), \quad \sigma_j = (-1)^j \quad (0 \le j \le 9). \end{aligned} \tag{53}$$

The elementary identity $P(\cos\phi) = \cos(9\phi)$ follows by expanding the cosine recurrence. It gives $P(s_j) = \sigma_j$ and $\max_{[-1,1]} |P| = 1$. The ten s_j are the simple roots of N. Since N has leading coefficient 256 and the roots are decreasing, $\operatorname{sign} N'(s_j) = \sigma_j$.

For $|t| \le \tau$, $U(t) \ge 3/5 - 7/15625 > 1/2$, by discarding the positive terms in its polynomial. Thus $N(t) < 0$. Also $\min_j |s_j| = \sin(\pi/18) > 1/9$ by strict concavity of sine, so $|s_j - t| > 1/90$. Define

$$\lambda(t) = -\frac{N'(t)}{N(t)} - \frac{a^2 t}{1 - a^2 t^2}, \qquad M(t) = P'(t) + \lambda(t) P(t). \tag{54}$$

Writing $\kappa = b_t'(t)/b_t(t) = -a^2 t/(1 - a^2 t^2)$, the functional $J_t Q = Q'(t) + \lambda(t) Q(t)$ satisfies $J_t(N/b_t) = 0$. For the cardinal polynomials $L_j(s) = N(s)/[(s - s_j)N'(s_j)]$, every polynomial V of degree at most ten has $V - \sum_j V(s_j) L_j$ equal to a constant times N. Divide this identity by b_t and apply J_t to obtain

$$J_t(V/b_t) = \sum_{j=0}^{9} d_j(t)(V/b_t)(s_j), \qquad d_j(t) = \frac{b_t(s_j)}{c_t} \frac{-N(t)}{(t - s_j)^2 N'(s_j)}. \tag{55}$$

The expression for d_j follows by differentiating $b_t(s_j) L_j(s)/b_t(s)$; the N' and b_t' terms cancel using the specified sign of κ. All denominators are nonzero and

$$\sigma_j d_j(t) > 0. \tag{56}$$

Theorem 5.1 (Full-space atomic representation)**.** *Under* (41)*, for every* $|t| \le 1/10$ *and every* $e \in \mathcal{V}_9$*, the functional*

$$J_{\theta,t}(e) = \frac{a}{c_t} E_r(\theta, r_t) + \lambda(t) E(\theta, r_t) \tag{57}$$

has the representation

$$J_{\theta,t}(e) = \sum_{j=0}^{9} d_j(t) \left[\frac{S_+(s_j)}{b_t(s_j)} e(Q_{s_j,-}) + \frac{S_-(s_j)}{b_t(s_j)} e(Q_{s_j,+}) \right]. \tag{58}$$

Its exact norm is

$$\|J_{\theta,t}\|_* = M(t) = \sum_{j=0}^{9} |d_j(t)| > 0. \tag{59}$$

The normalized original multipliers are $\lambda_r = \lambda(t)/M(t)$ *and* $\mu_r = a/(c_t M(t)) > 0$*.*

Proof. Apply (55) to the degree-ten numerator in (52). The two matching data there identify its left-hand side with (57). At the contact nodes $q_t(s_j) > 0$, so both conditional weights are positive. The signed measure in (58) has total variation at most $\sum_j |d_j|$. All its points lie in T_η, so this bounds the dual norm.

The global polynomial $p_*(x,y,z) = P(z/a)$ belongs to $\mathcal{V}_9$ and has $\|p_*\|_{T_\eta} = 1$. At both points of level s_j it equals σ_j. Therefore

$$J_{\theta,t}(p_*) = \sum_j d_j\sigma_j = \sum_j |d_j| = P'(t) + \lambda(t)P(t) = M(t) > 0.$$

This proves saturation and hence (59). Points at different levels cannot coincide. If two points at the same level coincide, their weights have the same sign and add, preserving total variation and saturation. The chain factor a/c_t is positive, giving the asserted sign of μ_r for both signs of t. □

The proof verifies the identity on a basis of the full 100-dimensional real space and uses the original tube norm. A positive combination of *signed contact evaluations* is not a functional positive on every nonnegative field.

5.1.5 Tangency, aggregation, and terminal positions

If (41) is strict, all twenty contact points are distinct. On its equality boundary, (44) shows that a discriminant vanishes only for $(s,t) = (-1,\tau)$ or $(1,-\tau)$. At that level $S_+ = S_- = b_t/2$, so the two half-weights form one atom. There are exactly nineteen atoms when $|t| = \tau$, and twenty when $|t| < \tau$. This statement applies at each angular centre whose chosen side has equality, including a terminal; it is not restricted to the angular midpoint.

Although the individual square roots may fail to be differentiable in parameters at tangency, the moment recurrence and rational expressions are regular because $b_t > 0$. Jet matching differentiates those moments, not the individual roots. At $t = 0$, separately, $\lambda(0) = 0$, $M(0) = 9$ and $\mu_r = a/9$; the value constraint remains present.

5.2 The objective estimate on the original geometry

We now prove the scalar estimate on the full parameter domain. Its geometric premise is precisely the support condition needed for Theorem 5.1; the scalar estimates themselves hold for every original geometry.

Lemma 5.2 (Uniform objective margin)**.** *For $|t| \le 1/10$, let $R = R_\theta(a^2t^2)$ and $S = S_\theta(a^2t^2)$. With* (54)*, $0 < M(t) < 24$, and*

$$\frac{9(S+\lambda(t)tR)}{M(t)} = \begin{cases} 1, & t = 0, \\ 1 + \dfrac{\Delta_\theta(t)}{M(t)} > 1 + \dfrac{111}{8}t^2, & 0 < |t| \le 1/10. \end{cases} \tag{60}$$

Here $\Delta_\theta(t) = 9(S+\lambda(t)tR) - M(t) > 333t^2$ off centre.

Proof. Put $x = t^2 \le 1/100$. The explicit polynomials give, for $t \ne 0$,

$$\tfrac{1}{2} < U \le 1, \qquad U - 1 \le x(-40 + 12/5 + 4/15625) < 0,$$
$$U'/t \le -80 + 48/5 + 32/15625 < 0,$$
$$0 < 39/5 - 9/15625 \le P/t < 9.$$

The lower bound on U was proved above; the lower bound on P/t discards its positive terms, while its upper bound uses $-120 + 108/25 + 4/15625 < 0$. Consequently

$$\frac{\lambda(t)}{t} = \frac{2}{1-x} - \frac{U'(t)/t}{U(t)} - \frac{a^2}{1-a^2x} > 2 - \frac{1}{64} = \frac{127}{64} > 0.$$

Also

$$0 < -tU'(t) = x(80 - 960x + 2688x^2 - 2048x^3) < 81x,$$

since $80 + 2688/10000 < 81$. It follows that $0 < \lambda(t)t < 3x + 162x = 165x$, and hence

$$0 < M(t) = 9U + (\lambda t)(P/t) < 9 + 1485x \le 477/20 < 24.$$

Using (33),

$$S - U \ge x(317/8 - 12/5 - 4/15625) > 37x,$$

$$9R - P/t \ge x(951/8 - 108/25 - 4/15625) > 114x.$$

The final strict inequalities follow respectively from $9/40 > 4/15625$ and $111/200 > 4/15625$. Since $\lambda t > 0$,

$$\Delta_\theta(t) = 9(S - U) + (\lambda t)(9R - P/t) > 333x.$$

Dividing by $0 < M < 24$ gives (60), because $333/24 = 111/8$. At $t = 0$, substitution gives $R = S = U = 1$, $P = \lambda = 0$ and $M = 9$, without division by t. This also proves the mass bound at the centre. The estimates use (33), which holds throughout the stated parameter domain. □

Corollary 5.3 (Certified pointwise lower bounds)**.** *Where* (41) *holds,*

$$D(\theta, r_t) > A_\theta(1 + 111t^2/8) \quad (0 < |t| \le 1/10), \qquad D(\theta, 0) = A_\theta. \tag{61}$$

Proof. For every feasible field, (59) and the positivity of a/c_t imply

$$\|e\|_{T_\eta} \ge -\frac{J_{\theta,t}(e)}{M(t)} \ge \frac{(a/c_t)F_r + \lambda(t)F}{M(t)} = \frac{aB(\theta)(S + \lambda(t)tR)}{M(t)}.$$

Take the infimum and use Lemma 5.2. The value constraint is an equality, so its transfer permits either sign of λ. The inequality uses the positive derivative multiplier; $\lambda t > 0$ was used in the scalar objective estimate. At $t = 0$ the lower bound is attained by the global field $e = -A_\theta P(z/a)$: its value is zero, its normal derivative is $-B(\theta)$, and its tube norm is A_θ. This proves the pointwise central equality, without classifying all its minimizers. □

6 Rigidity and exact stability regimes

6.1 Central rigidity and two support regimes

6.1.1 Central rigidity, including its angular boundary

The central rigidity argument includes an available side of length exactly 2δ by distinguishing the auxiliary chord from the locations of its actual contact atoms.

Lemma 6.1 (A closed angular-side condition gives central rigidity)**.** *Fix $\theta_0 \in I$. If one of its available angular sides has length $b_* \ge 2\delta$, then*

$$D(\theta_0, 0) = A_{\theta_0}, \qquad e = -A_{\theta_0} p_* \quad \textit{is its unique minimizer in } \mathcal{V}_9.$$

Proof. Write $\varepsilon \in \{-1, 1\}$ for the direction of the available side and $\ell = |\alpha|$ for an auxiliary chord angle. At $t = 0$ the kernel has

$$b_0(s) = 1, \qquad q_0(s) = \frac{a^2 s^2}{4\sin^2(\ell/2)}, \qquad S_\pm(s) = \frac{1 \pm \sqrt{1 - 4q_0(s)}}{2}.$$

Reality for every $|s| \le 1$ needs only $\ell \ge 2\delta$. The coordinates $z = as$ and $1 + S_{\pm}(e^{i\varepsilon\ell} - 1)$ give points on the sphere, since their horizontal squared modulus is $1 - a^2 s^2$. At $\ell = 2\delta$ the ten contact levels $s_j = \cos(j\pi/9)$ are all nonzero, hence $0 < S_-(s_j) \le S_+(s_j) < 1$. Every contact therefore has angle strictly between θ_0 and $\theta_0 + 2\varepsilon\delta$, even if that is the entire available side. At $s_j = \pm 1$ the roots coincide at $1/2$, with angular offset $\varepsilon\delta$; these normal-side points are included in the tube. Aggregation gives eighteen atoms, distinct from the nineteen-atom tangencies on the strip boundary.

There are finitely many contact levels. By continuity their angles remain in the physical side for every $2\delta < \ell < 2\delta + \epsilon < \pi/4$, for some $\epsilon > 0$, even when the auxiliary chord endpoint lies beyond that side. The roots remain real for all $|s| \le 1$. The moment and interpolation identities are identities for global polynomial fields on the sphere; their algebra does not require the intermediate, noncontact points to lie in the tube. Only the atoms used to bound the functional by the tube norm must lie there, as just proved.

For completeness, at $t = 0$ the conditional moments obey $m_0 = 1$, $m_1 = 2q_0$, and $m_n = m_{n-1} - q_0 m_{n-2}$. Thus $\deg m_n \le n + 1$, and $m_n(0) = m_n'(0) = 0$ for $n \ge 1$. On every Fourier–z basis element the averaged function has degree at most ten and derivative $aE_r(\theta_0, 0)$ at zero. Its interpolation remainder at the ten levels is a multiple of the even polynomial $N(s) = (s^2 - 1)U_8(s)$, whose derivative at zero vanishes. The same coefficients

$$d_j = \frac{-N(0)}{s_j^2 N'(s_j)}, \qquad \operatorname{sgn} d_j = (-1)^j$$

therefore represent $a\ell_{(\theta_0,0)}$ for all the chord angles just described. The two conditional weights are positive, and evaluation on $p_* = T_9(z/a)$ shows that the mass and norm are exactly $\sum_j |d_j| = T_9'(0) = 9$. This proves the lower cost A_{θ_0}; the field $-A_{\theta_0} p_*$ attains it with value zero.

Normalize any minimizer by $h = -e/A_{\theta_0}$. Then $\|h\|_{T_\eta} = 1$ and $a\,\partial_r(h \circ X)(\theta_0, 0) \ge 9$ by feasibility; the norm of the functional forces equality. In each representation every signed contact value equals one, since their positive weighted sum equals its full mass. Put $z_j = as_j$, $R_j = \sqrt{1 - z_j^2}$. The farther contact has angular offset $\varepsilon\Psi_j(\ell)$, where

$$\Psi_j(\ell) = \frac{\ell}{2} + \arccos\frac{\cos(\ell/2)}{R_j}, \qquad \Psi_j'(\ell) = \frac{1}{2} + \frac{\sin(\ell/2)}{2\sqrt{\sin^2(\ell/2) - z_j^2}} > 0.$$

This follows by rotating the chord by $-\varepsilon\ell/2$; its real part becomes $\cos(\ell/2)$. For $\ell > 2\delta$ in the above interval every farther contact traces an open angular arc within the tube. Thus $h - p_*$ vanishes on an arc at each of the ten heights z_j. At fixed height it is a trigonometric polynomial of degree at most nine, so it vanishes on the entire latitude. In (51) the coefficient at frequency m has a polynomial factor of degree at most $9 - m$, times the nonzero factor $(1 - z^2)^{m/2}$. Ten distinct roots force every coefficient to vanish. Hence $h = p_*$ on the sphere. □

6.1.2 A uniform side throughout the sector

If

$$\sin(L/4) \ge W(a), \tag{62}$$

choose $\alpha = L/2$ for $\theta \le (\eta + \omega)/2$ and $\alpha = -L/2$ otherwise. Every chosen segment lies in I and (41) holds. Thus the central bound (61) applies at every angle, and the barrier (38) covers $|t| \ge 1/10$. Both bounds apply at $|t| = 1/10$. The side selection may jump at the angular midpoint, but both choices represent the same functional and exact norm; no

globally continuous selection of atoms is asserted. Since B has its minimum on I at an endpoint, these two overlapping bounds imply the global lower bound

$$d_\eta \geq \frac{a}{9} \min\{B(\eta), B(\omega)\}. \tag{63}$$

The single-maximum property of B follows from the derivative computed immediately before Proposition 4.4.

Condition (62) is necessary and sufficient for reality of all intersections of this particular uniform-side construction: if it fails, $(s,t) = (-1, 1/10)$ has negative discriminant for each chosen side. This does not exclude other certificates or imply a smaller nodal-stability radius. Moreover $W(a) > a = \sin\delta$, so (62) implies $L > 4\delta$, even on its equality boundary. In particular Lemma 6.1 applies at every centre, using a side of length at least $L/2 > 2\delta$.

6.1.3 A local side and a closed target margin

Let $\eta < \theta_c < \omega$ and suppose

$$\sin((\omega - \theta_c)/2) \geq W(a), \qquad \min\{B(\theta_c), B(\omega)\} \geq 2\cos(\delta/2) B(\eta). \tag{64}$$

For $\theta \in [\eta, \theta_c]$ choose $\alpha = \omega - \theta$. The first condition qualifies the atomic construction on this entire zone, including its cutoff, both strip edges and support tangencies. The outer barrier covers $|t| \geq 1/10$. The second condition supplies the target margin on the complementary angular zone, with its closed boundary treated separately below.

In the open second zone (θ_c, ω) strict unimodality gives $B(\theta) > \min\{B(\theta_c), B(\omega)\}$. Proposition 4.5 therefore gives $D > A_\eta$. At either endpoint $\theta = \theta_c, \omega$ the strict off-centre floor gives the same conclusion for $r \neq 0$. For the two remaining centres note that $W(a) > a = \sin\delta$, so $\omega - \theta_c > 2\delta$. From θ_c the side toward ω is long enough for Lemma 6.1; from ω the side toward η has length $L > 2\delta$. It follows that $D(\theta_c, 0) = A_{\theta_c} > A_\eta$ and $D(\omega, 0) = A_\omega > A_\eta$, since $2\cos(\delta/2) > 1$. We have proved, including the equality in the target margin,

$$D(\theta, r) > A_\eta \quad (\theta_c \leq \theta \leq \omega,\ |r| \leq \delta). \tag{65}$$

Thus no atom construction is needed to cover the open second zone; the two endpoint centres use only the central cost lemma. A strict lower bound of $\sqrt{65}B(\eta)/4$ or a lower bound of $2B(\eta)$ for $\min\{B(\theta_c), B(\omega)\}$ each implies the target-margin condition in (64).

On $[\eta, \theta_c]$ strict unimodality and $B(\theta_c) > B(\eta)$ give $B(\theta) > B(\eta)$ for $\eta < \theta \leq \theta_c$. The central-strip certificate and outer barrier then show

$$d_\eta \geq A_\eta. \tag{66}$$

The closed regions overlap at θ_c and the normal bounds overlap at $|t| = 1/10$; no unexamined seam remains. The support premise already implies $L > 2\delta$ and does not require $L > 4\delta$.

The plotted case is qualified without numerical sampling: $\eta < 1/100$ and $\omega > 2/5$ imply $L > 39/100$, whence $\sin(L/4) > 9/100$, whereas $W(a) < 11\eta/40 < 11/4000$. Also $\delta < 1/8$ gives $\sin(3\delta/2) > (11/10)\delta > W(a)$ and $3\delta < L$. Thus both the uniform regime and the inset side are admissible. For these parameters $\sin(2\eta) < 1/50$ and $B(\omega) = 3/625$, so $B(\eta) < (1/50)^3/64 < 3/625 = B(\omega)$. Thus η is the minimizing terminal used in Figure 2.

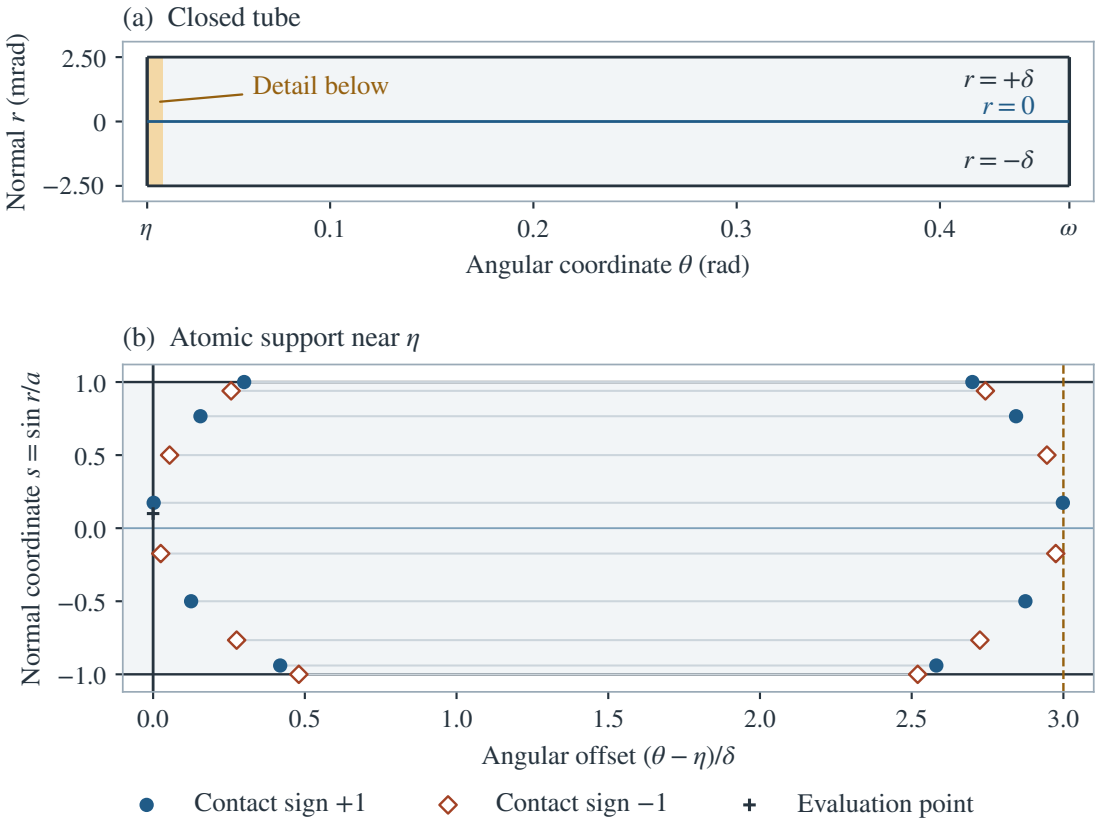

Figure 1: The tube and an explicit supported jet, in coordinate charts. Here $\eta = \arctan(1/100)$, $\omega = \arctan(1/2)$. (a) The full angular interval and signed normal distance, with independent axis scales; this is not an isometric development of the sphere. (b) The twenty signed contacts of Theorem 5.1 at $\theta_0 = \eta$, $t = 1/10$, using $\alpha = 3\delta$, in coordinates $((\theta - \eta)/\delta, \sin r/a)$. The signs label the functional weights. The support count is not asserted minimal, and the drawing is not a norm certificate.

6.2 Exact radii and behaviour at equality

6.2.1 Classifying all minimizing pairs

Under L, the strip certificate and the outer barrier give $D(\theta, r) > A_\theta$ whenever $r \neq 0$. At $r = 0$, every angle has an available side of length at least $L/2 > 2\delta$, so Lemma 6.1 gives $D(\theta, 0) = A_\theta$ with the unique field $-A_\theta T_9(z/a)$. Since B has no interior minimum, the minimizing points are exactly the terminal centres that realize β. The minimum cost is A_* and all those points have the same unique minimizing field e_C. This includes a tie between the two terminal fibres.

Under M, (65) excludes the entire second zone. In the first zone the same two bounds exclude $r \neq 0$, and $B(\theta) > B(\eta)$ for $\theta > \eta$ excludes the other centres. Lemma 6.1 applies at η, giving the only minimizing pair $((\eta, 0), e_C)$ and cost $A_\eta = A_*$. In both cases Proposition 4.4 identifies this cost with ρ_η.

6.2.2 The critical graph and the closed ball

Proposition 6.2 (The critical field and every amplification)**.** *For every original geometry the only zeros of $f + e_C$ in the tube are $r = 0$. At any terminal where $B = \beta$, the defining level has zero spherical gradient there. For every $\gamma > 1$, $f + \gamma e_C$ has at least three distinct interior zeros on each such terminal fibre.*

Proof. The identity

$$1 - \frac{T_9(t)}{9t} = t^2 H(t^2), \qquad H(u) = \frac{40}{3} - 48u + 64u^2 - \frac{256}{9}u^3$$

extends continuously to $t = 0$. Its derivative satisfies $H'(u) = -(256/3)(u - 3/4)^2 \leq 0$, so $H(u) \geq H(1) = 8/9$ for $0 \leq u \leq 1$. Using $B \geq \beta$ and the positive target bound yields, for $r > 0$ and $t = \sin r/a$,

$$\frac{F + E_C}{\sin r} = B(\theta) R_\theta(a^2 t^2) - \beta \frac{T_9(t)}{9t} \geq \frac{55}{72}\beta t^2 > 0. \tag{67}$$

Oddness gives the opposite sign for $r < 0$. Along the centre, the angular derivative is zero and the normal derivative is $B(\theta) - \beta$, proving the gradient assertion.

On a terminal with $B = \beta$, the field $F + \gamma E_C$ vanishes at the centre with derivative $(1 - \gamma)\beta < 0$. It is negative just to its right. At $t_0 = \sin(\pi/9) \in (0, 1)$, the first positive zero of T_9, its value equals the strictly positive F. The intermediate value theorem gives another positive zero strictly between the centre and t_0. Oddness gives a negative zero as well. This argument places no upper bound on γ and does not use normal-side signs. □

Completion of Theorem 2.3. The general bounds and the exact-jet identity were proved in Propositions 4.4, 4.5 and 4.2. The preceding classification proves the exact L/M radii and all their minimizing pairs. If a field of norm at most $A_* < j_\eta$ failed P_η, then Corollary 3.7 would supply a feasible oriented jet. Its norm would have to equal the minimum A_*, and the field would have to be e_C. But Proposition 6.2 shows that e_C preserves the graph. The entire closed ball is therefore safe. The fields γe_C have norms γA_* and fail for every $\gamma > 1$; as γ decreases to one their costs approach A_*. Thus the failure infimum is not attained in these regimes. □

The critical graph is smooth although its defining level is singular at the minimizing terminals. The attainment of the jet minimum is therefore compatible with nonattainment of actual graph failure. Outside the proven exact regimes, e_C still preserves the graph and its amplifications still fail, but A_* need not be the true failure radius.

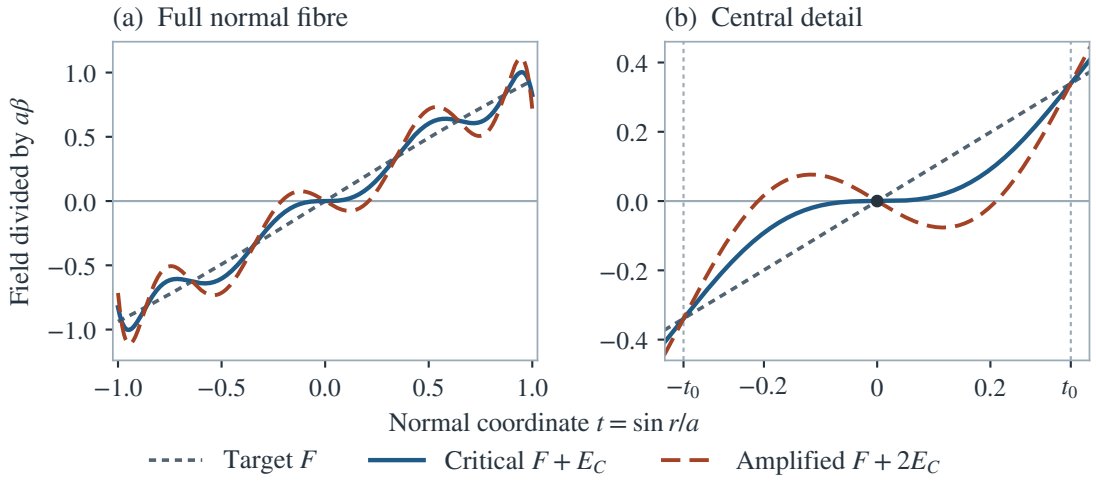

Figure 2: The terminal fibre $\theta = \eta$ for the same geometry as Figure 1. The horizontal coordinate is $t = \sin r/a$; values are divided by $a\beta$. Curves show the target F and the perturbed fields $F + \gamma E_C$ with $\gamma = 1, 2$. The second panel enlarges the central interval. The guides $t = \pm\sin(\pi/9)$ are zeros of T_9, used as sign witnesses in Proposition 6.2; they are not the outer roots of the amplified field. The curves illustrate the continuous proof; the conclusion of at least three zeros follows from the proposition.

7 Two examples separating a criterion from a formula

7.1 A valid radius beyond the uniform support condition

Example 7.1 (An adapted sector beyond L)**.** Let

$$\eta = \arctan(1/100), \qquad L = \frac{21}{5}\delta, \qquad \omega = \eta + L, \qquad \theta_c = \eta + \frac{3}{2}\delta. \tag{68}$$

Then (62) fails but (64) holds. Hence $\rho_\eta = A_\eta$ with the unique critical field and safe closed ball of Theorem 2.3.

Proof. Here $\tan\delta = 25/10001$, so

$$\eta < 1/100, \qquad \delta < 1/400, \qquad \omega < 41/2000 < \pi/6.$$

In particular the original domain holds. Since $\arctan x \geq x/(1+x^2)$ for $x > 0$ (integrate the decreasing function $(1+s^2)^{-1}$),

$$\delta > \frac{25/10001}{1 + (25/10001)^2} > \frac{3}{1250} > \frac{6\eta}{25}.$$

Thus $\theta_c > 34\eta/25 > 4\eta/3$. Also $a > (99/100)\delta$ and $a^2 < 1/10$, using $\sin x \geq x - x^3/6$ and $\delta < 1/400$. Therefore

$$\sin(L/4) < \frac{21}{20}\delta < \frac{1089}{1010}\delta < \frac{11a}{10 + a^2} = W(a),$$

which violates the uniform support test, without saying anything yet about the radius.

For the adapted side, $\omega - \theta_c = 27\delta/10$. On $0 \leq u \leq 27\delta/20$, $\cos u > 9/10$, giving

$$W(a) < \frac{11}{10}\delta < \frac{243}{200}\delta < \sin(27\delta/20).$$

This proves the first M premise. For $\theta \in [\theta_c, \omega]$, $2\theta < 1/20$. The elementary sine and cosine estimates give

$$\frac{\sin(2\theta)}{2\theta} > \frac{2399}{2400}, \qquad \cos(2\theta) > \frac{799}{800}.$$

Since $(2399/2400)^3 > 799/800$ and $(799/800)^2 > 399/400$, while $B(\eta) < \eta^3/8$,

$$\frac{B(\theta)}{B(\eta)} > \left(\frac{\theta}{\eta}\right)^3 \frac{399}{400} > \left(\frac{4}{3}\right)^3 \frac{399}{400} = \frac{532}{225} > 2 > 2\cos(\delta/2).$$

This verifies the closed M margin, with room to spare, at both endpoints and on the whole second zone. The stated theorem applies. □

7.2 A narrow sector where the formula is false

The next construction changes the geometry, not the perturbation space or its continuous norm. Its degree-six correction exploits the small variation of a field between very close terminal fibres.

Example 7.2 (A strict upper bound below the central candidate)**.** Let

$$\tan\omega = \frac{1}{2}, \qquad \tan\eta = \frac{499999999}{10^9}. \tag{69}$$

There is an explicit $e_* \in \mathcal{V}_9$ and an explicit positive U such that

$$G_{e_*}(\eta, 0) = \partial_r G_{e_*}(\eta, 0) = 0, \qquad \|e_*\|_{T_\eta} \le U < A_\eta = A_*.$$

Furthermore $\rho_\eta \le U < A_*$. This is a strict upper bound. The exact radius and whether a genuine graph failure attains it remain open.

Proof. Write $\mathcal{T}(z) = T_9(z/a)$ and, for $i = 0, \dots, 4$, set

$$s_i = \cos(i\pi/9), \quad z_i = a s_i, \quad u_i = \sqrt{1 - z_i^2}, \quad b = \sqrt{1 - a^2}, \quad \nu = \prod_{i=0}^{4} (1 - u_i) > 0.$$

The symbol ν is distinct from the jet minimum d_η. Define the global real polynomial of degree six

$$H(x, y, z) = z \prod_{i=0}^{4} (x\cos\eta + y\sin\eta - u_i). \tag{70}$$

It is odd in z. On the terminal fibre let $H_0(z) = z\prod_{i=0}^{4}(\sqrt{1 - z^2} - u_i)$. Then $H_0'(0) = \nu$.

Put $\Delta(z) = \prod_{i=0}^{4}(\sqrt{1 - z^2} + u_i) \ge (2b)^5$ for $|z| \le a$. Factoring the five differences, and using the eight roots of the Chebyshev derivative, gives

$$\mathcal{T}'(z) = \frac{2304}{a^9} \prod_{i=1}^{4} (z^2 - z_i^2), \qquad H_0(z) = \frac{a^9 z (a^2 - z^2) \mathcal{T}'(z)}{2304 \Delta(z)}.$$

Here derivatives are with respect to z. The Chebyshev identity $1 - \mathcal{T}(z)^2 = (a^2 - z^2)\mathcal{T}'(z)^2/81$ and $|z|\sqrt{a^2 - z^2} \le a^2/2$ imply

$$|H_0(z)| \le C\sqrt{1 - \mathcal{T}(z)^2}, \qquad C = \frac{a^{11}}{512(2b)^5}. \tag{71}$$

Consequently, for $\epsilon > 0$, $|\mathcal{T} + \epsilon H_0| \le \sqrt{1 + \epsilon^2 C^2}$. This last inequality follows from the Cauchy–Schwarz inequality in two dimensions, including the contact points.

At a general point of the tube, $x\cos\eta + y\sin\eta = \sqrt{1-z^2}\cos(\theta - \eta) \in [0,1]$. On $[0,1]$ the derivative of $\prod_{i=0}^{4}(u - u_i)$ has absolute value at most five, since each factor has absolute value at most one. The mean value theorem therefore gives

$$|H - H_0| \le h, \qquad h = 5a(1 - \cos L) \le \frac{5}{2}aL^2 \tag{72}$$

on the entire closed tube. Suppose for the moment that $L^2 < 2\nu/45$. Then the constants

$$g = \frac{a\nu}{9} - h > 0, \qquad \epsilon = \frac{g}{C^2}, \qquad K = \frac{9}{a} + \epsilon\nu$$

are positive. Define

$$e_* = -\frac{B(\eta)}{K}(\mathcal{T}(z) + \epsilon H(x,y,z)). \tag{73}$$

Since $z_r = 1$ at the centre, this field has the stated exact jet at $(\eta, 0)$. Equations (71) and (72), together with $\sqrt{1+x} \le 1 + x/2$ for $x \ge 0$, give

$$\begin{aligned} \|e_*\|_{T_\eta} \le U &:= \frac{B(\eta)}{K}[1 + \epsilon(h + g/2)] \\ &= A_\eta\left[1 - \frac{\epsilon g}{2(1 + \epsilon a\nu/9)}\right] < A_\eta. \end{aligned} \tag{74}$$

The identity uses $\epsilon C^2 = g$ and $a\nu/9 = h + g$. This continuous estimate does not substitute a sampled maximum.

It remains to check the small-width condition for the exact parameters (69). Put $\alpha = 499999999/10^9$. Since the derivative of arctangent is at most one, $0 < L \le 10^{-9}$. Moreover

$$a = \frac{\alpha}{\sqrt{16(1+\alpha^2)^2 + \alpha^2}} > \frac{1}{16},$$

because $\alpha > 3/8$ and its displayed denominator is less than six. The double-angle identity gives $\cos(\pi/9)\cos(2\pi/9)\cos(4\pi/9) = 1/8$; with $\cos(\pi/3) = 1/2$ this yields $\prod_{i=0}^{4} s_i = 1/16$. Hence

$$\nu \ge \prod_{i=0}^{4}\frac{a^2 s_i^2}{2} = \frac{a^{10}}{8192} > 2^{-53}, \qquad L^2 \le 10^{-18} < \frac{2^{-52}}{45} < \frac{2\nu}{45},$$

where the middle comparison is the integer inequality $45 \cdot 2^{52} < 10^{18}$. This proves the required hypothesis.

Finally $\omega = \arctan(1/2) < \pi/6$, so $\beta = B(\eta)$. For any $1 < \gamma < A_\eta/U$, $\|\gamma e_*\|_{T_\eta} \le \gamma U < A_\eta < j_\eta$. The field $F + \gamma E_*$ has zero value and negative normal derivative $(1-\gamma)B(\eta)$ at the terminal centre. It is odd in r on that fibre, and the strict side signs give one additional interior zero on each side of the centre. Thus these are genuine failures. Letting $\gamma \downarrow 1$ gives $\rho_\eta \le U < A_\eta$. The construction is global, and its norm estimate and failure argument apply continuously on the whole tube. □

8 Conditioning and its critical limit

8.1 Quantitative control below the radius

Throughout this section the geometry in (2) is fixed. The constants may depend on both angular endpoints. We first make the regularity of the pointwise cost D from Section 4.1 explicit, then quantify the graph control.

Proposition 8.1 (Lipschitz continuity of the pointwise cost)**.** *Equip the closed rectangle D_η with Euclidean distance in (θ, r) coordinates. There are finite constants L_0, L_1 such that*

$$|D(p) - D(q)| \le \left(L_0 + \frac{2aL_1}{\cos\delta}\right)|p - q| \qquad (p, q \in D_\eta). \tag{75}$$

One may take

$$L_0 = \max_{\|e\|_{T_\eta} \le \|f\|_{T_\eta}} \max_{D_\eta} |\nabla_{\theta,r} G_e|_2, \qquad L_1 = \max_{\|e\|_{T_\eta} \le \|f\|_{T_\eta}} \max_{D_\eta} |\nabla_{\theta,r} \partial_r G_e|_2.$$

Proof. The field $-f$ is feasible at every point, so $D(p) \le \|f\|_{T_\eta}$. The coefficient sublevel $\|e\|_{T_\eta} \le \|f\|_{T_\eta}$ is compact by Lemma 3.4. The field and its derivatives depend continuously on these coefficients and on the point, hence both displayed maxima are finite. The rectangle is convex, so the mean value estimate along its coordinate segments applies with L_0, L_1.

Choose a minimizer e_p at p. Write $q = (\theta_q, r_q)$ and $[u]_+ = \max(u, 0)$. The globally defined field

$$\widehat{e} = e_p - G_{e_p}(q) - \frac{[\partial_r G_{e_p}(q)]_+}{\cos r_q}(z - \sin r_q) \in \mathcal{V}_9$$

satisfies $G_{\widehat{e}}(q) = 0$ and $\partial_r G_{\widehat{e}}(q) = \min(\partial_r G_{e_p}(q), 0)$. Because $G_{e_p}(p) = 0$ and $\partial_r G_{e_p}(p) \le 0$,

$$|G_{e_p}(q)| \le L_0|q - p|, \qquad [\partial_r G_{e_p}(q)]_+ \le L_1|q - p|.$$

Moreover z ranges over $[-a, a]$ on the tube, so $\|z - \sin r_q\|_{T_\eta} = a + |\sin r_q| \le 2a$ and $\cos r_q \ge \cos\delta$. The triangle inequality gives $D(q) \le D(p) + (L_0 + 2aL_1/\cos\delta)|q - p|$. Interchanging p, q proves the claim, including all four sides. □

These constants are existence bounds on a fixed compact family, not certified numerical values or bounds uniform as $\eta \downarrow 0$. This regularity concerns the outer minimization $d_\eta = \min_p D(p)$; it does not interchange that minimum with the fixed-point dual maximum.

For the slope estimate define another finite operator norm,

$$M_\theta = \max_{\|e\|_{T_\eta} \le 1} \max_{D_\eta} |\partial_\theta(e \circ X)|, \qquad L_F = \frac{47}{15}(\cot\eta + \tan\omega) + 2\tan(2\omega). \tag{76}$$

Compactness as above proves finiteness of M_θ, and homogeneity gives $\|\partial_\theta E\|_\infty \le M_\theta \|e\|_{T_\eta}$. No numerical value of M_θ is claimed here.

Lemma 8.2 (Relative angular derivative of the target)**.** *On the entire closed tube, $|\partial_\theta F| \le L_F|F|$.*

Proof. For $r \ne 0$, put $c = \cos\theta$, $s = \sin\theta$ and $Q = \tan^2 r$. The product formula for F gives

$$\partial_\theta \log|F| = \cot\theta - \tan\theta - 2\tan(2\theta) - \frac{2sc}{c^2 - Q} + \frac{2sc}{s^2 - Q}.$$

As in Lemma 3.1, $Q \le c^2 s^2/16$, so $c^2 - Q \ge 15c^2/16$ and $s^2 - Q \ge 15s^2/16$. Taking absolute values therefore bounds this logarithmic derivative by $(47/15)(\cot\theta + \tan\theta) + 2\tan(2\theta) \le L_F$. At $r = 0$ both F and $\partial_\theta F$ vanish identically, which completes the proof without division at a node. □

Proposition 8.3 (Normal margin, position and slope)**.** *Let $0 \le m < d_\eta = \rho_\eta$ and $\|e\|_{T_\eta} \le m$. Then e has a unique graph h, and at every node $p = (\theta, h(\theta))$,*

$$\partial_r G_e(p) \ge \frac{\cos h(\theta)}{a + |\sin h(\theta)|}(D(p) - m) \ge \kappa := \frac{\cos \delta}{2a}(d_\eta - m) > 0. \tag{77}$$

Furthermore,

$$\|h\|_\infty \le \frac{2m}{\beta}, \qquad h' = -\frac{\partial_\theta G_e}{\partial_r G_e}\Big|_{r=h}, \qquad \|h'\|_\infty \le \frac{m(L_F + M_\theta)}{\kappa}. \tag{78}$$

The derivatives at angular terminals are one-sided.

Proof. Since $m < d_\eta < j_\eta$, the side signs are strict and every zero has positive normal derivative: otherwise e would be feasible for the definition of d_η. The graph argument already proved in Section 3.3 applies. At any node $p = (\theta, r)$ write $g = \partial_r G_e(p) > 0$. The global affine correction

$$q_p(x, y, z) = -\frac{g}{\cos r}(z - \sin r)$$

belongs to the degree-at-most-one subspace of $\mathcal{V}_9$. It preserves the zero and cancels its normal derivative. Its exact norm is

$$\|q_p\|_{T_\eta} = \frac{g}{\cos r}(a + |\sin r|).$$

Thus $D(p) \le \|e + q_p\|_{T_\eta} \le m + \|q_p\|_{T_\eta}$, which proves the pointwise inequality and, using $D(p) \ge d_\eta$, the uniform one.

At the graph $|F(\theta, h)| = |E(\theta, h)| \le m$. Integrating $\partial_r F > \beta/2$ from zero to h yields the position bound. The implicit function theorem and (77) give the derivative identity. Lemma 8.2 bounds $|\partial_\theta F|$ there by $L_F m$, and (76) bounds $|\partial_\theta E|$ by $M_\theta m$. At a terminal the field extends to an open chart neighborhood and the same theorem gives a local smooth graph; restricting to I justifies the stated one-sided derivative. □

This proof uses positivity only at the nodes, not monotonicity of the perturbed field throughout the tube. Outside L and M, d_η is still the variational value, not an evaluated number. Within either exact regime one can replace it by A_*. The bound on slope grows like the inverse of the available margin; no optimality of this general estimate is asserted.

Corollary 8.4 (Closed additive budget in an exact regime)**.** *Assume L or M, $0 \le m < A_*$ and $\|e\|_{T_\eta} \le m$. For every $q \in \mathcal{V}_9$ with $\|q\|_{T_\eta} \le A_* - m$, the field $f + e + q$ still has the graph property. This includes equality, but does not guarantee a strictly positive normal derivative at equality.*

Proof. The triangle inequality gives $\|e + q\|_{T_\eta} \le A_*$, and Theorem 2.3 applies to the closed ball. For the final caution take $e = (m/A_*)e_C$ and $q = (1 - m/A_*)e_C$. Their sum is e_C, whose normal derivative vanishes at each minimizing terminal, while its graph remains $r = 0$. □

8.2 A smooth field limit with divergent graph slope

We now work in either exact regime L or M and keep its geometry fixed. The following family separates uniform graph convergence from control of the terminal slope.

Theorem 8.5 (Loss of C^1 conditioning from inside the ball)**.** *For $0 < \varepsilon < 1$ set*

$$e_\varepsilon = (1-\varepsilon)e_C + \frac{\varepsilon A_*}{2}. \tag{79}$$

Then

$$\|e_\varepsilon\|_{T_\eta} = (1-\varepsilon/2)A_* < A_*, \qquad \|e_\varepsilon - e_C\|_{T_\eta} = \frac{3}{2}\varepsilon A_*. \tag{80}$$

The fields converge to e_C in $C^k(S^2)$ for every fixed nonnegative integer k. Their unique graphs satisfy

$$\|h_\varepsilon\|_\infty \le \frac{a}{\cos\delta}\left(\frac{12\varepsilon}{55}\right)^{1/3} \longrightarrow 0. \tag{81}$$

For each minimizing terminal θ_*, including both in an L tie, put

$$c_1(\theta) = 4 + \frac{1}{\sin^2\theta\cos^2\theta}, \qquad C_* = \frac{40}{3} - a^2 c_1(\theta_*) > 0.$$

Then $B'(\theta_*) \neq 0$ and, as $\varepsilon \downarrow 0$,

$$h'_\varepsilon(\theta_*) = \frac{aB'(\theta_*)(18C_*)^{1/3}}{3\beta C_*}\varepsilon^{-1/3}(1 + O(\varepsilon^{1/3})). \tag{82}$$

The derivative is in increasing θ, with its one-sided meaning at a terminal. In particular the graph map from the closed A_* ball, with the tube norm, to $C^1(I)$ is discontinuous at e_C, even along fields strictly inside the ball.

Proof. The entire interval $[-1,1]$ is attained by $t = z/a$ on each fibre. Since T_9 attains both -1 and 1, the range of e_ε/A_* is $[-1+3\varepsilon/2, 1-\varepsilon/2]$. For $0 < \varepsilon < 1$ its largest absolute value is $1-\varepsilon/2$. Also $(e_\varepsilon - e_C)/(\varepsilon A_*) = T_9(z/a) + 1/2$ has norm $3/2$. This proves (80). The difference is ε times a fixed smooth global field, which proves the stated C^k convergence.

Let $G_C = F + e_C \circ X$ and $t_\varepsilon(\theta) = \sin h_\varepsilon(\theta)/a$. Theorem 2.3 and Proposition 8.3 give the unique graphs and their positive normal derivatives, including the terminal interpretation of the implicit function theorem. The critical sign bound (67) and oddness give

$$|G_C(\theta, r)| \ge \frac{55}{72}a\beta|t|^3.$$

At a zero of G_{e_ε}, on the other hand, $|G_C| = \varepsilon A_*|T_9(t_\varepsilon) + 1/2| \le 3\varepsilon A_*/2$. Thus $|t_\varepsilon|^3 \le 12\varepsilon/55$ uniformly on I. Since $|\sin h| \ge \cos\delta\,|h|$ for $|h| \le \delta$, (81) follows.

The only critical point of B in $(0, \pi/4)$ is its strict maximum $\pi/6$, by (39). It cannot minimize on the nondegenerate interval I; consequently $B'(\theta_*) \neq 0$ at each minimizing terminal. From the coefficient bound behind (33), $a^2 c_1(\theta_*) < 1/8$, so $C_* > 0$.

Before restricting to a graph, the polynomial formula (32) reads

$$F(\theta, r) = aB(\theta)t(1 - a^2 c_1(\theta)t^2 + O(t^4)), \qquad T_9(t) = 9t - 120t^3 + O(t^5).$$

The remainders here come from polynomials in t with smooth coefficients on the fixed interval I. They may therefore be differentiated as polynomial expressions before the zero is inserted. At $\theta = \theta_*$ the cancellation $B(\theta_*) = \beta$ yields

$$\frac{G_{e_\varepsilon}(\theta_*, r)}{a\beta} = C_* t^3 + \frac{\varepsilon}{18} + \varepsilon t + O(t^5 + \varepsilon|t|^3). \tag{83}$$

At $t = t_\varepsilon(\theta_*)$, the previously proved $|t| = O(\varepsilon^{1/3})$ now gives

$$t^3 = -\frac{\varepsilon}{18C_*} + O(\varepsilon^{4/3}), \qquad t = -\left(\frac{\varepsilon}{18C_*}\right)^{1/3}(1 + O(\varepsilon^{1/3})).$$

The perturbation is independent of θ. Differentiating the field formulas first, with $\partial_r t = \cos r/a$, gives

$$\partial_\theta G_{e_\varepsilon}(\theta_*, r) = aB'(\theta_*)t + O(t^3), \tag{84}$$

$$\partial_r G_{e_\varepsilon}(\theta_*, r) = \beta \cos r\big(3C_* t^2 + O(t^4 + \varepsilon)\big). \tag{85}$$

At the zero, the error in the second parentheses is $O(\varepsilon^{1/3})$ relative to $3C_*t^2$; $\cos h_\varepsilon = 1 + O(\varepsilon^{2/3})$. Substituting these estimates into $h' = -G_\theta/G_r$ proves (82), including its sign. In a terminal tie it is positive at η and negative at ω. Its nonzero coefficient forces $\|h'_\varepsilon\|_\infty \to \infty$, whereas the critical graph is identically zero. This proves the discontinuity into $C^1(I)$ despite (81). □

All constants and remainders in this theorem refer to the fixed tube. This is not the limit $\eta \downarrow 0$ at fixed ω. Along this path $A_* - \|e_\varepsilon\|_{T_\eta} = \varepsilon A_*/2$; the proved $\varepsilon^{-1/3}$ slope divergence neither asserts nor refutes optimality of the general inverse-margin upper bound in (78).

9 Singularity, bandwidth and observable boundaries

9.1 Two singular events in the closed tube

Let d_{n} be the least tube norm of a field $e \in \mathcal{V}_9$ with $G_e = \partial_r G_e = 0$ somewhere in D_η, and let d_{s} be the infimum for a zero of $f + e$ at which the full spherical gradient also vanishes, with the point restricted to T_η. Then

$$d_{\mathrm{n}} = d_\eta, \qquad d_\eta \le d_{\mathrm{s}} \le A_*; \qquad d_{\mathrm{n}} = d_{\mathrm{s}} = A_* \quad \text{in L or M.} \tag{86}$$

Indeed, the first identity is Proposition 4.2. A full singular zero is also a feasible normal jet, proving the lower bound. For the upper bound, Proposition 6.2 gives $G_C(\theta, 0) = 0$ for every θ and $\partial_r G_C(\theta_*, 0) = B(\theta_*) - \beta = 0$ at each minimizing terminal. Hence $\partial_\theta G_C$ vanishes there too. The chart metric $dr^2 + \cos^2 r\, d\theta^2$ is nonsingular, so these two vanishing components give a zero spherical gradient, including at the boundary of the tube. The same field has norm A_*. In L/M both singular events are attained at this norm, while the failure infimum of the graph has the same value and is not attained. No equality $d_{\mathrm{s}} = d_\eta$ outside these regimes is inferred.

If the singular point may lie anywhere on the sphere, the distance is instead zero already for $e = 0$. At $(1, 0, 0)$ the target and its ambient gradient vanish: both factors y and z vanish in the product (1). This point is outside the chosen tube. Thus a global discriminant distance is a different question.

9.2 A globally smooth counterexample outside the band

For $\ell > 0$ define on the whole sphere

$$e_\ell(x, y, z) = -\frac{3\beta}{2}\ell \sin(z/\ell). \tag{87}$$

These are real smooth global fields with $\|e_\ell\|_{\infty,S^2} \le 3\beta\ell/2 \to 0$. At a minimizing terminal θ_*, the pullback of $f + e_\ell$ is odd in r, vanishes at zero and has derivative $B(\theta_*) - 3\beta/2 = -\beta/2 < 0$ there. For sufficiently small ℓ, $3\beta\ell/2 < j_\eta$, so the side values keep their opposite signs. The intermediate value theorem then gives an additional positive and negative zero on that fibre. The graph fails for arbitrarily small value norms in this larger class.

The fields (87) are not in $\mathcal{V}_9$. To see this, suppose a polynomial of degree at most nine restricted to the sphere represented one of them. Average it under rotations about the z axis. The represented field is unchanged, while the averaged polynomial restricts to a polynomial in z of degree at most nine: surviving terms are constants times $z^k(1-z^2)^j$ with $k + 2j \le 9$. But $\sin(z/\ell)$ cannot agree with a polynomial on $[-1, 1]$, by analyticity, a contradiction. The positive band-limited radius therefore cannot be transferred to arbitrary smooth errors measured only by their values.

9.3 Signed fields, complex modulus and temporal RMS

Take a peak phasor $U = f + i\epsilon$ with $\epsilon > 0$ and the real temporal field

$$u(x, \tau) = \mathrm{Re}(U(x)e^{i\nu\tau}), \qquad \nu \neq 0.$$

Its signed real component at $\tau = 0$ is f, with the original nodal set. In contrast $|U| = \sqrt{f^2 + \epsilon^2} \ge \epsilon$ has no zero. If $T = 2\pi/|\nu|$ and N is a positive integer, the RMS over any N complete periods is

$$\left(\frac{1}{NT} \int_{\tau_0}^{\tau_0 + NT} u(x, \tau)^2 \, d\tau \right)^{1/2} = \frac{|U(x)|}{\sqrt{2}} > 0.$$

On any other positive-duration interval the RMS is still positive, although that simple formula need not hold: a nonzero sinusoid cannot vanish identically on such an interval. The nonzero-frequency condition matters; at zero frequency the imaginary part is not observed by the displayed real temporal field. These distinctions concern specified mathematical observables. They do not convert this tube norm into a pressure tolerance, a deposition law or a material response.

10 Discussion and reproducibility

The variational reduction answers which event controls the local graph: simultaneous cancellation of the value and normal derivative determines the radius throughout the original domain, and normal-side escape costs more. The spherical certificate makes this answer explicit in the uniform and adapted regimes. It also identifies the unique critical field and shows that a minimum-cost singular level can still define a single smooth graph. The genuine graph-failure infimum has the same value but is not attained in these regimes.

The two examples delimit that answer in different ways. The adapted sector retains the exact radius beyond the uniform support condition; the narrow sector has a rigorously smaller failure radius than the Chebyshev candidate. Its exact radius is not evaluated here. The general pointwise cost away from the centre and the maximal geometry of validity of the candidate formula remain analytic questions. The conditioning theorem establishes a separate boundary: a fixed positive margin gives graph estimates, whereas convergence to the critical field can produce divergent slopes at the minimizing terminals. The compactness constants in those estimates have no certified numerical values in this work and are not asserted uniform under degeneration of the tube.

10.1 A companion with fixed inputs

The accompanying directory `companion/` is an autonomous finite-check package. Its `README.md` records the exact input parameters, dependencies, commands and output identities for the adapted-sector and narrow-sector checks. It includes a proof/source map, the selected input records, the check scripts and the figure generator. The two generated PDFs are in `paper/figures/` in the public repository. The companion runs independently of the laboratory application and its stored simulations.

The checks evaluate prescribed symbolic and rational identities; the normal and optimized Python modes are compared on the same fixed inputs. They are not searches for a support or for a better radius. In particular, selected record checks and finite algebraic identities do not establish the continuous admissibility, signs, rigidity or norm bounds by themselves. Those arguments are contained in the proofs above. The two figures sample explicit formulas for illustration and do not certify a continuous maximum. The companion records the scope of each check separately from the theorem it accompanies.

10.2 Scope of the geometric conclusion

All radius statements concern the real degree-at-most-nine band, the specified normalization and the complete closed tube. They do not describe global nodal topology or guarantee stability for arbitrary smooth errors. A real component, a complex amplitude and a temporal RMS are different observables, as the explicit examples show. Establishing a relation to a physical response would require its own model, admitted inputs and evidence. The present result provides a precise geometric stability question, a finite-dimensional variational characterization, exact regimes and proved obstructions within that question.

Acknowledgement. The preparation of this manuscript and its computational companion used AI assistance.

A Why the polynomial space is the full spherical band

Here is an elementary justification of the equality in (4). Write $R^2 = x^2 + y^2 + z^2$. If p_n is homogeneous of degree n, a direct product-rule calculation gives, for a homogeneous polynomial q_m of degree m,

$$\Delta(R^{2k} q_m) = 2k(2m + 2k + 1) R^{2k-2} q_m + R^{2k} \Delta q_m. \tag{88}$$

Put $N = \lfloor n/2 \rfloor$, $a_0 = 1$, and

$$a_k = -\frac{a_{k-1}}{2k(2n - 2k + 1)} \quad (1 \le k \le N), \qquad H_n = \sum_{k=0}^{N} a_k R^{2k} \Delta^k p_n.$$

Equation (88) cancels adjacent terms in ΔH_n; the final derivative $\Delta^{N+1} p_n$ is zero. Thus H_n is homogeneous and harmonic of degree n, and $p_n - H_n$ is divisible by R^2. Repeating on the quotient expresses p_n as a sum of R^{2k} times homogeneous harmonic polynomials of degrees $n - 2k$. On the unit sphere $R = 1$, so every ambient polynomial of degree at most nine restricts to the sum of spherical harmonics of degrees at most nine. The reverse inclusion is immediate.

The sum is direct. The radial Laplacian formula, obtained by the chain rule in polar coordinates, is

$$\Delta(R^\ell Y) = R^{\ell-2}\big(\ell(\ell+1)Y + \Delta_{S^2}Y\big).$$

A degree-ℓ harmonic restriction therefore has spherical Laplacian eigenvalue $-\ell(\ell+1)$. These eigenvalues are distinct. Applying the product of the other corresponding linear factors in Δ_{S^2} to a vanishing sum separates each component and shows that it is zero. Proposition 3.3 then gives the total dimension 100 without assuming a smaller symmetry class. This is a reconstruction of the standard harmonic decomposition, not a novelty claim.

References

[1] Oleg Davydov and Robert Schaback. Minimal numerical differentiation formulas. *Numerische Mathematik*, 140:555–592, 2018. DOI; locators refer to arXiv:1611.05001v2.

[2] Mareike Dressler, Simon Foucart, Mioara Joldes, Etienne de Klerk, Jean-Bernard Lasserre, and Yuan Xu. Least multivariate Chebyshev polynomials on diagonally determined sets. *SIAM Journal on Applied Algebra and Geometry*, 10(2):450–466, 2026. DOI; locators refer to the author manuscript v3 (also arXiv:2405.19219v3).

[3] Tamás Erdélyi. Basic polynomial inequalities on intervals and circular arcs. *Constructive Approximation*, 39:367–384, 2014. DOI; locators refer to the 18-page author manuscript.

[4] Khazhgali Kozhasov, Bernard Mourrain, and Adam Parusiński. On the distance to discriminants and osculating varieties. arXiv:2610.06538v1, 2026. Version of 5 October 2026.

[5] Antonio Lerario and Michele Stecconi. What is the degree of a smooth hypersurface? *Journal of Singularities*, 23:205–235, 2021. DOI; publisher PDF.

[6] Christophe Raffalli. Distance to the discriminant. arXiv:1404.7253v3, 2014. Version of 18 June 2014.